ACS OMEGA

http://pubs.acs.org/journal/acsodf

Perspective

Achieving Complexity at the Bottom: Molecular Metamorphosis Generated by Anthocyanins and Related Compounds

Nuno Basílio, A. Jorge Parola, Diogo Sousa, Vesselin Petrov, Luis Cruz, Victor de Freitas, and Fernando Pina*

Cite This: *ACS Omega* 2021, 6, 30172–30188

Read Online

ACCESS | Metrics & More | Article Recommendations

ABSTRACT: The concept of molecular metamorphosis is described. A molecule (flavylium cation) generates a sequence of other different molecules by means of external stimuli. The reversibility of the system allows for the flavylium cation to be recovered by other external stimuli, completing one cycle. Differently from supramolecular chemistry, molecular metamorphosis is not a bottom-up approach. All events occur at the bottom. The procedures to characterize the kinetics and thermodynamics of the cycles are summarized. They are based on direct pH jumps (addition of a base to the flavylium cation) and reverse pH jumps (addition of an acid to equilibrated solutions at higher pH values). Stopped flow is an indispensable tool to characterize these systems. The following metamorphic cycles will be described to illustrate the concept: (i) introducing the flavanone in the metamorphic system and illustrating the concept of a timer at the molecular level; (ii) response of the flavylium-based metamorphosis to light inputs and the write-lock-read-unlock-erase molecular system; (iii) a one-way cycle of direct−reverse pH jumps; (iv) interconversion of the flavylium cation with 2,2′-spirobis[chromene] derivatives; (v) 6,8 A-ring substituent rearrangements.

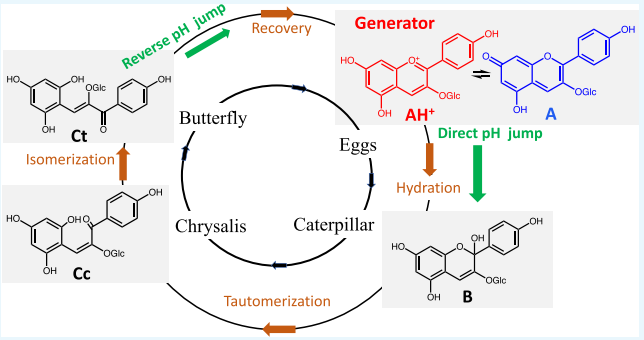

1. INTRODUCTION

Complexity is an intrinsic characteristic of biological systems. The top-down approach is the most common way to investigate complexity. Examples of this procedure are separation techniques such as chromatography, distillation, evaporation, and filtration, experimental procedures that, for example, allow the discovery of new molecules in natural products.

In contrast, supramolecular chemistry, a discipline well-established and recognized after the 1987 Nobel Prize awarded to Donald J. Cram, Jean-Marie Lehn, and Charles J. Pedersen, is based on a bottom-up approach (Scheme 1). Supramolecular chemistry studies how molecules interact to give higher dimension entities and tends to fill the gap between "classical chemistry" and biology[1] (Scheme 1).

However, there is another way to achieve complexity. The molecular metamorphosis[2] defines the situation of a molecule (generator) capable by external inputs of giving a different molecule and another one successively, leading to a set of new molecules. The complexity results from the number of species, and everything takes place at the bottom. Anthocyanins, the ubiquitous color systems of angiosperms reported in Scheme 2, provide a paradigmatic example of chemical metamorphosis.[2,3]

A molecule, the red flavylium cation, the sole species at pH ≤ 1, can generate, upon a pH input (addition of a base defined as a direct pH jump), the purple quinoidal base (proton transfer) and successively the colorless hemiketal (hydration), which is

Scheme 1. Top-Down and Bottom-Up Approaches[a]

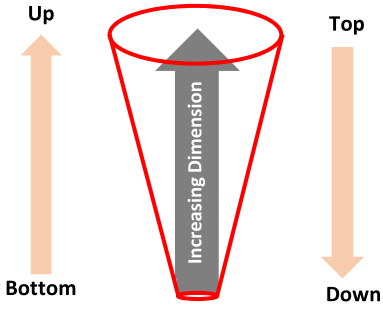

[a]Increasing of the dimension is a characteristic of the bottom-up approach.

Received: August 18, 2021
Accepted: October 4, 2021
Published: October 13, 2021

Scheme 2. Multistate of Chemical Species of Cyanidin-3-glucoside (Kuromanin) in Acidic to Neutral Aqueous Solutions[a]

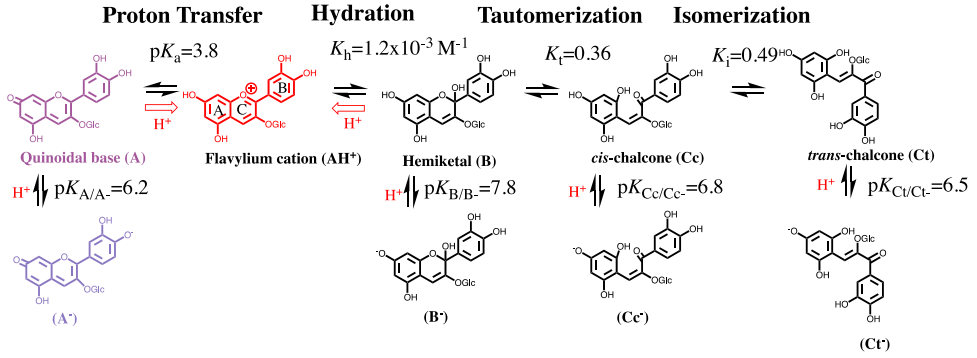

[a] $K_x = k_x/k_{-x}$ (X = **A**, **B**, **CC**, and **Ct**).

transformed into the pale yellow *cis*-chalcone (tautomerization) and finally *trans*-chalcone (isomerization) (Schemes 2 and 3).

Scheme 3. Analogy between Zoological Metamorphosis and Pelargonidin-3-glucoside Molecular Metamorphosis[a]

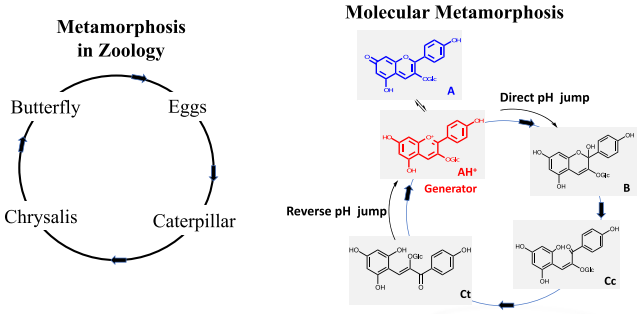

[a] This system is ubiquitous in anthocyanins and related compounds. The characteristics of the molecular metamorphosis systems are very dependent on the substitution pattern as shown through this work.

One characteristic of the system consists of its reversibility. The flavylium cation can be recovered by addition of an acid back to pH ≤ 1 (defined as reverse pH jumps). The fact that in molecular metamorphosis, different molecules are formed implies the appearance of new physical chemical properties caused by external inputs. It is possible to profit from this fact to design molecular sensors,[4,5] models for optical memories,[6,7] and drug delivery based on host−guest chemistry,[8,9] among other applications.

Strictly, the term metamorphosis means a change of the form or nature of a thing or person into a completely different one. In fact, all chemistry can be considered to be a metamorphosis phenomenon. We use chemical metamorphosis in a more restricted sense by considering the analogy with its zoological significance (Scheme 3).

To overcome the false dilemma "which came first: the chicken or the egg?" in defining the generator molecule in anthocyanin-based metamorphosis cycles, it is preferable to consider the flavylium cation: not only it is the most stable species, but also, it gives the name to the system. However, the identification of the complex system with its generator could give rise to some misunderstandings in studies where the anthocyanin complexity is not taken into account.

The term "aromatic metamorphosis" has been applied to the substitutions of the endocyclic atoms in aromatic cores (regarded as being uncleavable because of their aromatic stabilization energy) through partial disassembly of the cyclic skeletons and subsequent ring reconstruction (Scheme 4). For

Scheme 4. Aromatic Metamorphosis Does Not Fit Our Concept of Molecular Metamorphosis.

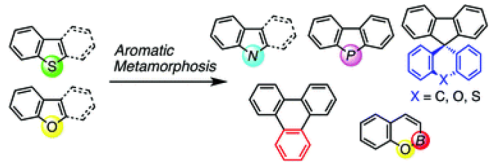

With Permission from Ref 10. Copyright 2017. Royal Society of Chemistry

example, dibenzothiophenes, dibenzofurans, and benzofurans are transformed into different ring systems.[10] Aromatic metamorphosis does not fit our concept of molecular metamorphosis in particular because it is not reversible and does not respond to an external input.

The concept of molecular metamorphosis is also different from a multiresponsive molecular switch.[11−13] Strictly, a molecular switch refers to a system with two states, ON/OFF, very appropriate for defining molecular logic gates.[14−17] In a multiresponsive molecular switch, the same molecule responds to more than one of external stimuli, such as pH, light, metal cations, and anions. There is no sequence of species as in Scheme 3.

2. MOLECULAR METAMORPHOSIS OF ANTHOCYANINS AND RELATED COMPOUNDS: KINETIC AND THERMODYNAMIC CHARACTERIZATION

The molecular metamorphosis system shown in Scheme 2 for cyanidin-3-glucoside (kuromanin) is conveniently characterized by an energy level diagram (Scheme 5).[6,18]

In this type of representation, the Gibbs free energy (ΔG^0) of each reaction of the first row of Scheme 2 is calculated and represented in a diagram as in Scheme 5.[6,19] For example, electron-donating substituents (such as amines and hydroxyl or alkoxy groups) attached to the flavylium core are known to provide stabilization to the flavylium cation against hydration (the **B** energy level increases).[3] The isomerization kinetics/thermodynamics is also affected by the substituents: functional groups that decrease the chalcone double bond character (such as electron-donating groups in position 7) lead to faster isomerization rates (lower activation barrier), and the opposite

https://doi.org/10.1021/acsomega.1c04456
ACS Omega 2021, 6, 30172−30188

Scheme 5. Energy Level Diagram of Cyanidin-3-glucoside.

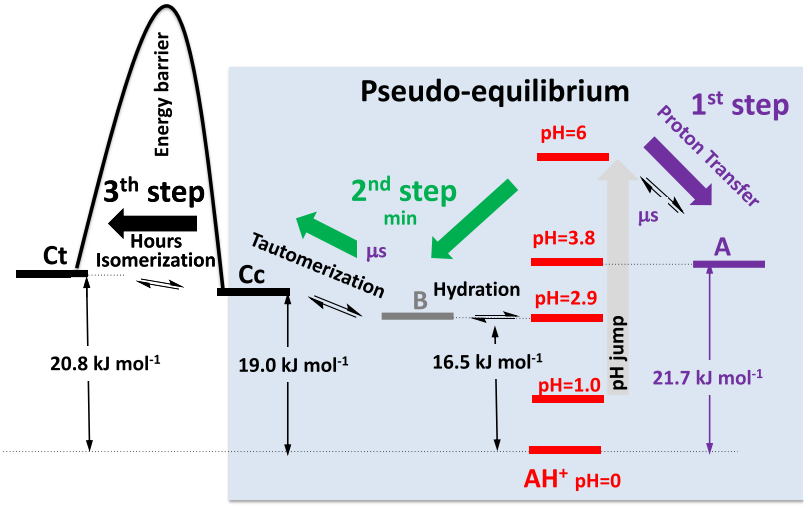

Adapted with Permission from Ref 18. Copyright 2021. MDPI

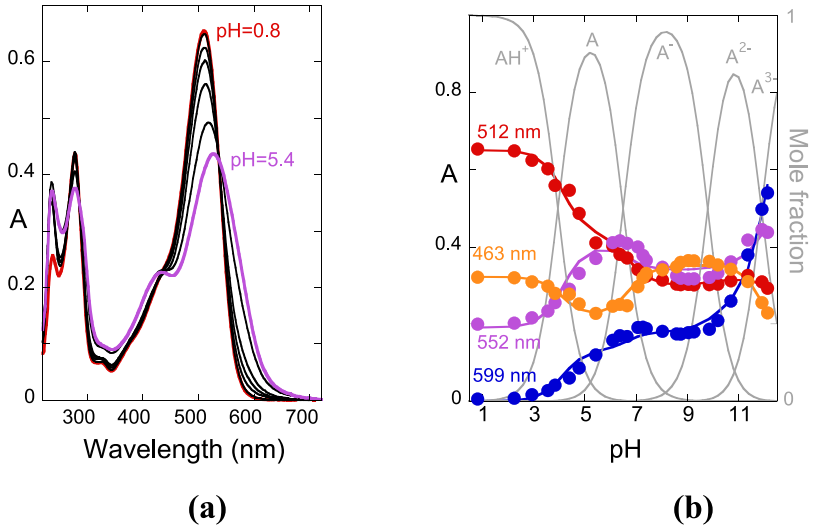

Figure 1. (a) Spectral variations of cyanidin-3-glucoside taken 10 ms after a direct pH jump to 0.8 < pH < 5.4 followed by stopped flow (pK_a = 3.8), before interference of the anionic species; (b) extension to higher pH values: representation of the absorbance at representative pH values versus pH; pK_{A/A^-} = 6.6; $pK_{A^-/A^{2-}}$ = 10.1; $pK_{A^{2-}/A^{3-}}$ = 12.1 form the absorption spectra taken 10 ms after a direct pH jump.

is observed for substituents that increase the charge density in the carbonyl group increasing the isomerization barrier (electron-donating groups in position 4′).[3] Also worth noting is the effect of substituents in position 4, which usually completely hinder the hydration of the flavylium cation such that for these compounds, only the colored flavylium and quinoidal base species are present in solution.[20]

As shown below, any effect affecting the kinetics and thermodynamics of the elemental reaction steps will be translated into overall pH-dependent stability (pK'_a and $pK^{\wedge}_a$) of the flavylium cation (pH flavylium domain) and the kinetics/mechanism of the multistate. In this sense, in many cases, the overall outcome for the introduction of substituents in particular positions of the flavylium skeleton may be difficult to predict.

2.1. Response of the Metamorphosis System of Anthocyanins and Related Compounds to pH Inputs. Let us consider the generator molecule flavylium cation, $\mathbf{AH}^+$, and the input direct pH jump, for the sake of simplicity up to a moderately acidic medium before formation of the anionic species. The first species to be formed is the quinoidal base, **A**, by proton transfer, eq 1, first step of Scheme 5. This reaction is by far the faster of the system and occurs during the mixing time of the stopped flow. The study of the first step requires very fast techniques, such as temperature jumps[21] or in some favorable cases flash photolysis profiting from the excited-state proton transfer of the flavylium cation.[22]

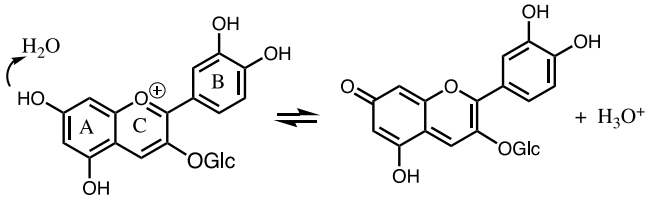

$$\mathbf{AH}^+ + H_2O \underset{k_{-a}}{\overset{k_a}{\rightleftharpoons}} \mathbf{A} + H_3O^+ \quad K_a \quad \text{proton transfer} \tag{1}$$

$$k_{1st(direct)} = k_a + k_{-a}[H^+] \tag{2}$$

https://doi.org/10.1021/acsomega.1c04456
ACS Omega 2021, 6, 30172−30188

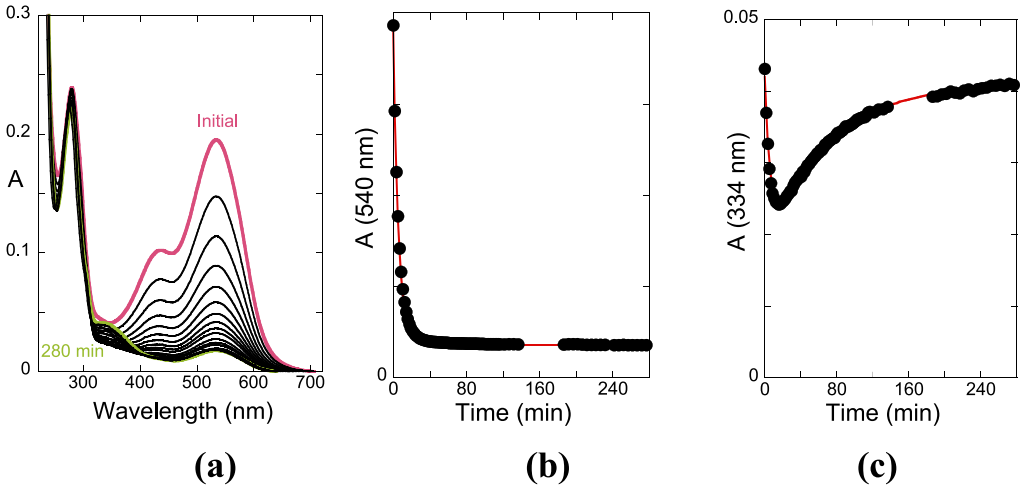

Figure 2. (a) Spectral variations corresponding to the second kinetic step after a direct pH jump from the flavylium cation, 1.9×10^{-5} M at pH = 1 to pH = 5.6; (b) trace of the disappearance of absorbance at 540 nm as a function of time, $k_{2nd} = 2.9 \times 10^{-3}$ s^{-1}; (c) third step evident following the trace at 334 nm where *trans*-chalcone absorbs, $k_{3rd} = 2.5 \times 10^{-4}$ s^{-1}.

During the subsequent much slower kinetic processes, **AH**$^+$ and **A** are in equilibrium and behave as a single species.

Despite the uselessness of the stopped flow to calculate the proton transfer rate constants of eq 1, the absorption spectra of **AH**$^+$ and **A** (as well as those of the anionic forms of **A**) can be achieved by collecting the absorption spectra after 10 ms after the direct pH jump (Figure 1). A pK_a = 3.8 was obtained by representing the absorbance as a function of pH.

The next step is the formation of a hemiketal, **B**, by hydration of the flavylium cation in position 2, eq 3.

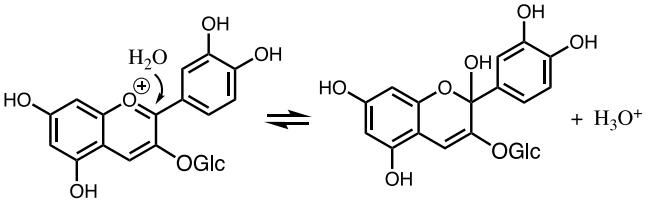

$$\mathbf{AH}^+ + 2H_2O \underset{k_{-h}}{\overset{k_h}{\rightleftharpoons}} \mathbf{B} + H_3O^+ \quad K_h \quad \text{hydration} \tag{3}$$

The hydration reaction, for the pH range accessed by direct pH jumps, is slower than the following kinetic step, the tautomerization reaction, eq 4, that corresponds to the opening/closure of ring C.

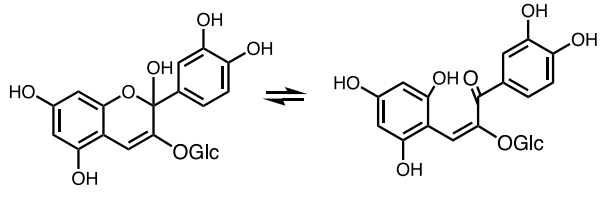

$$\mathbf{B} \underset{k_{-t}}{\overset{k_t}{\rightleftharpoons}} \mathbf{Cc} \quad K_t \quad \text{tautomerization} \tag{4}$$

The large difference in the rates of eqs 3 and 4 and the fact that the next and last step (isomerization) is much slower than all the others make hydration the rate-controlling reaction of the second step, eq 5 and Scheme 5, and permit the establishment of the equilibrium between **B** and **Cc**.

$$k_{2nd(direct)} = \chi_{AH^+} k_h + \chi_B k_{-h}[H^+] = \frac{[H^+]}{[H^+] + K_a} k_h + \frac{1}{1 + K_t} k_{-h}[H^+] \tag{5}$$

Here, χ_{AH^+} and χ_B are the mole fraction of **AH**$^+$ in its equilibrium with **A** and the mole fraction of **B** in its equilibrium with **Cc**, respectively.

In anthocyanins and many other related compounds, the *cis*–*trans* isomerization is by far the slowest step of the system, and consequently, during the isomerization, **AH**$^+$, **A**, **B**, and **Cc** are in equilibrium and behave as a single species (like **AH**$^+$ and **A** during the hydration/tautomerization above).[23] We define the pseudo-equilibrium as a transient state reached before significant formation of *trans*-chalcone (Scheme 5).

$$\mathbf{AH}^+ + H_2O \rightleftharpoons \mathbf{CB}^{\wedge} + H_3O \quad K_a^{\wedge} = K_a + K_h + K_h K_t \tag{6}$$

$$\mathbf{CB}^{\wedge} = [\mathbf{A}] + [\mathbf{B}] + [\mathbf{Cc}] \tag{7}$$

It is straightforward to prove by a mass balance and expressing all species in terms of **AH**$^+$ through the respective equilibrium constants, eqs 1, 3, and 4, that this system behaves as a single acid–base equilibrium with constant $K_a^{\wedge}$, eqs 6 and 7.[23]

The equilibrium is attained, the third step of Scheme 5, by the slow *cis*–*trans* isomerization, eqs 8 and 9, where χ_{Cc} is the mole fraction distribution of **Cc** at pseudo-equilibrium.

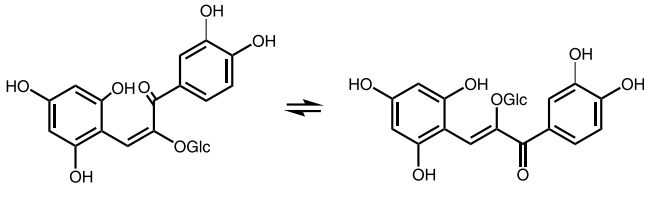

$$\mathbf{Cc} \underset{k_{-i}}{\overset{k_i}{\rightleftharpoons}} \mathbf{Ct} \quad K_i \quad \text{isomerization} \tag{8}$$

$$k_{3rd(direct)} = \chi_{Cc} k_i + k_{-i} = \frac{K_h K_t}{[H^+] + K_a + K_h + K_h K_t} k_i + k_{-i} \tag{9}$$

https://doi.org/10.1021/acsomega.1c04456
ACS Omega 2021, 6, 30172−30188

At equilibrium, the system also behaves as a single acid−base reaction as represented in eqs 10 and 11.

$$\mathbf{AH}^+ + H_2O \rightleftharpoons \mathbf{CB} + H_3O^+$$

$$K'_a = K_a + K_h + K_hK_t + K_hK_tK_i \quad (10)$$

$$\mathbf{CB} = [\mathbf{A}] + [\mathbf{B}] + [\mathbf{Cc}] + [\mathbf{Ct}] \quad (11)$$

The spectral variations corresponding to the second and third kinetic steps are shown in Figure 2.

The third step corresponds to the appearance of **Ct** exhibiting an absorption band centered around 334 nm, whose formation is visible in Figure 2c. In anthocyanins, **Ct** and **A** are minor species, and the major one is the hemiketal.

The spectral variations of cyanidin-3-glucoside at equilibrium are represented in Figure 3. In this pH range, the flavylium cation behaves as a single monoprotic acid in equilibrium with **CB**, eq 10, $pK'_a = 2.7 \pm 0.1$.

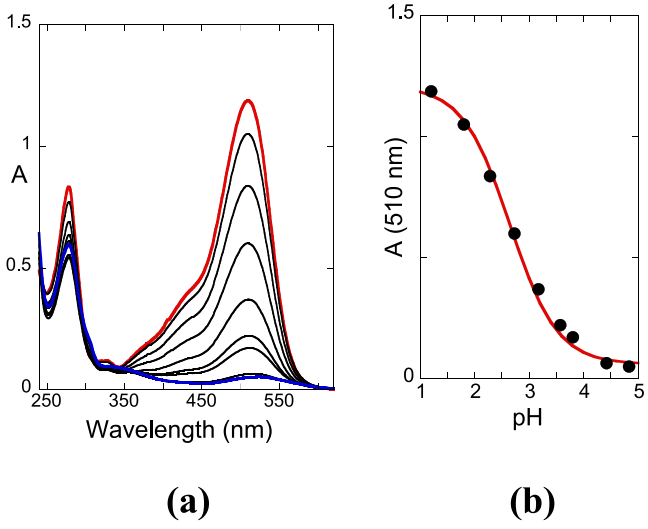

Figure 3. (a) Spectral variations of 2.3×10^{-5} M kuromanin upon direct pH jumps after 1 day. In this pH range, the flavylium cation behaves as a single monoprotic acid in equilibrium with **CB** (eq 10). (b) Fitting achieved for $pK'_a = 2.7 \pm 0.1$.

The molecular metamorphosis is not exclusive for anthocyanins. Other natural compounds generated by the flavylium cation of anthocyanidins, 3-deoxyanthocyanidins, auronidins like riccionidin A, and a variety of synthetic flavylium compounds, including styrylflavylium and furanoflavylium compounds (Scheme 6), generate molecular metamorphosis.

The system generated by some synthetic flavylium cations is much more robust than the one of anthocyanins in particular in a basic medium and very appropriate for applications in particular in photochromic systems.

2.1.1. Extension to the Basic Region. The extension of the system to the basic region is indispensable to understand how the molecular metamorphosis system based on anthocyanins confers blue colors to angiosperms but also to some applications based on synthetic generators as those shown in Scheme 6. In neutral to basic media, the hydroxyl substituents can deprotonate as shown in Scheme 1, leading to the anionic derivatives whose equilibrium constants are defined below.

For the first deprotonation,

$$\mathbf{X} + H_2O \rightleftharpoons \mathbf{X}^- + H_3O^+ \quad K_{X/X^-} = \frac{[X^-][H^+]}{[X]} \quad (12)$$

For the second deprotonation,

$$\mathbf{X}^- + H_2O \rightleftharpoons \mathbf{X}^{2-} + H_3O^+ \quad K_{X^-/X^{2-}} = \frac{[X^{2-}][H^+]}{[X^-]} \quad (13)$$

with **X** = **A**, **B**, **Cc**, and **Ct**.

The system can be simplified considering the flavylium cation to be a polyprotic acid by adding eqs 14 and 15 to eq 10.[24]

$$\mathbf{CB} + H_2O \rightleftharpoons \mathbf{CB}^- + H_3O^+$$

$$K''_a = [K_{A/A^-}K_a + K_{B/B^-}K_h + K_{Cc/Cc^-}K_hK_t + K_{Ct/Ct^-}K_hK_tK_i]/K'_a \quad (14)$$

$$\mathbf{CB}^- + H_2O \rightleftharpoons \mathbf{CB}^{2-} + H_3O^+$$

$$K'''_a = [K_{A^-/A^{2-}}K_{A/A^-}K_a + K_{B^-/B^{2-}}K_{B/B^-}K_h + K_{Cc^-/Cc^{2-}}K_{Cc/Cc^-}K_hK_t + K_{Ct^-/Ct^{2-}}K_{Ct/Ct^-}K_hK_tK_i]/K'_aK''_a \quad (15)$$

2.2. Reverse pH Jumps: A New Paradigm to Calculate the Equilibrium Constants. Reverse pH jumps carried out from the pseudo-equilibrated solutions at higher pH values back to flavylium at pH = 1.0, monitored by stopped flow, are a

Scheme 6. Families of Flavylium and Related Compounds Capable of Generating Molecular Metamorphosis

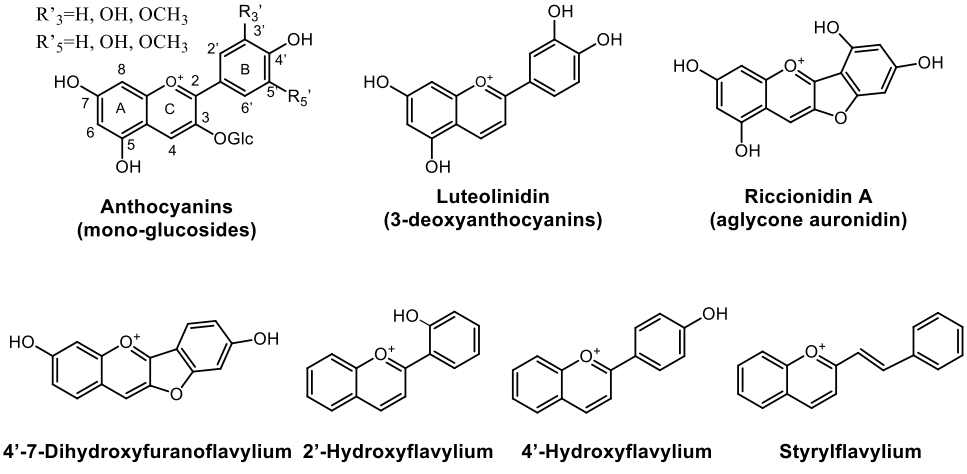

https://doi.org/10.1021/acsomega.1c04456
ACS Omega 2021, 6, 30172−30188

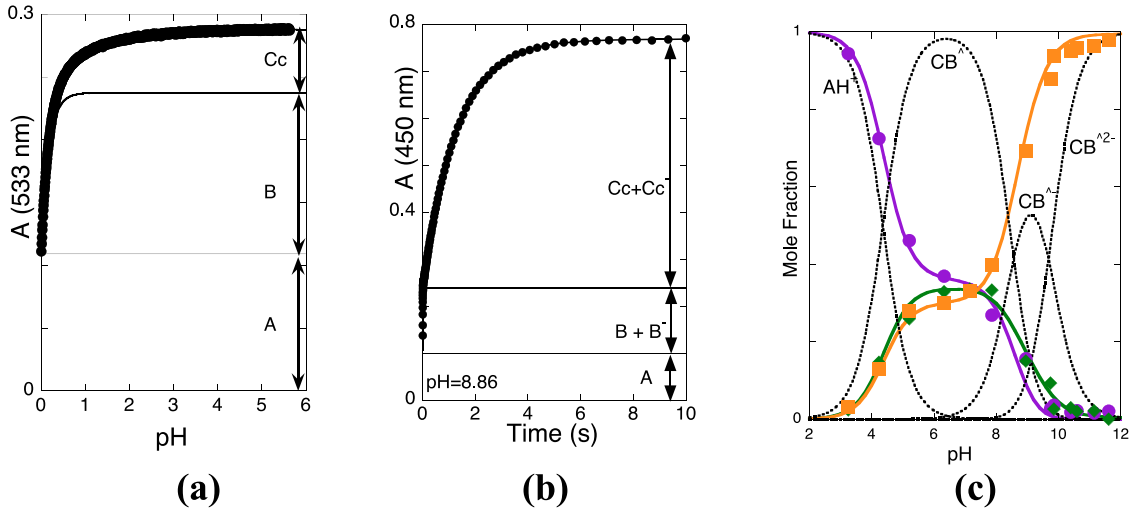

Figure 4. Stopped flow traces after reverse pH jumps of 4′-hydroxyflavylium from pH = 3.85 (a) and 8.86 (b) back to pH = 1. (c) Representation of the mole fractions of 4′-hydroxyflavylium taken from the normalized amplitudes of several experiments like those of (a) and (b) extended to the basic region.[24] $[\mathbf{CB}^{\wedge -}] = [\mathbf{B}^-] + [\mathbf{Cc}^-]$ and $[\mathbf{CB}^{\wedge 2-}] = [\mathbf{B}^{2-}] + [\mathbf{Cc}^{2-}]$ (anionic species of **A** are not possible in this compound). Reprinted with permission from ref 24. Copyright 2019. American Chemical Society.

powerful tool to study the molecular metamorphosis generated by flavylium cations (Figure 4c).[24,25] They are based on the change of the regime, taking place at a very acidic medium when the hydration (which is directly proportional to the proton concentration), eq 5, becomes faster than tautomerization. The compound 4′-hydroxyflavylium was selected to describe this procedure because it exhibits a long-lived pseudo-equilibrium with similar mole fractions of the species **A**, **B**, and **Cc**. The trace of stopped flow experiments is shown in Figure 4a.

The reverse pH jumps of the stopped flow have three components (Figure 4a,b): (i) the amplitude for $t = 0$ corresponds to the fraction of **A** that is converted into $\mathbf{AH}^+$ during the mixing time of the stopped flow together with $\mathbf{AH}^+$ that exists prior to the jump for lower pH values, (ii) the amplitude of the faster kinetic step corresponds to all **B** species because the anionic **B** forms are transformed into **B** during the mixing time of the stopped flow, and (iii) *mutatis mutandis* for the slower amplitude that gives the mole fraction of **Cc** and its anionic forms.

The rate constant of the faster kinetic trace (in an acidic medium) is accounted for by eq 16.

$$k_{\text{Hydr. rever. to pH=1}} = \chi_{\mathbf{AH}^+} k_h + k_{-h}[H^+] = \frac{[H^+]}{[H^+] + K_a} k_h + k_{-h}[H^+] \quad (16)$$

This equation is different from eq 5 because the formation of $\mathbf{AH}^+$ from **B** is faster and there is no time to establish the tautomerization equilibrium.

B is consumed to give $\mathbf{AH}^+$, during the faster kinetics of the stopped flow. The remaining **Cc** leads to more $\mathbf{AH}^+$, via **B** during the slower reaction. The observed rate is not dependent on k_t because there is no **B** available to give **Cc** by a back reaction. As soon as **B** is formed from **Cc**, it immediately gives $\mathbf{AH}^+$. In this case, the process follows eq 17, with k_{-t} defined above in eq 4 and k_{-t}^{H} the rate constant of tautomerization catalysis, previously defined by McClelland and coworkers.[25,26]

$$k_{3^{rd}(\text{stopped flow})} = k_{-t} + k_{-t}^{H}[H^+] + k_{-t}^{OH}[OH^-] \quad (17)$$

Fitting was achieved for $k_{-t} = 0.084\ s^{-1}$, $k_{-t}^{H} = 62\ M^{-1}\ s^{-1}$, and $k_{-t}^{OH} = 8.9 \times 10^{10} M^{-1}\ s^{-1}$. The last parameter is a rough estimate because for pH > 3.5, it is not possible to separate the two kinetics (see Figure 5d) and define with precision the ascending branch of the tautomerization curve in a basic medium (Figure 5c). The magnitude of the rate constant, k_{-t}^{OH}, indicates that this process should be controlled by diffusion as previously reported by McClelland and Gedge for similar compounds.[25]

In this regard of the direct pH jumps to the basic region, the respective rate constants are directly proportional to $[OH^-]$ concentration, according to eq 18.

$$k_{OH^- \text{ attack}} = k_{OH}[OH^-] \quad (18)$$

When considering the total pH range of the pseudo-equilibrium of 4′-hydroxyflavylium, the system behaves as a triprotic acid, *i.e.*, with $[\mathbf{CB}^{\wedge -}] = [\mathbf{B}^-] + [\mathbf{Cc}^-]$ and $[\mathbf{CB}^{\wedge 2-}] = [\mathbf{B}^{2-}] + [\mathbf{Cc}^{2-}]$ (anionic species of A are not possible in this compound), eq 19, and the respective mole fractions are given by eq 20.

$$\mathbf{AH}^+ \underset{[H^+]}{\overset{K_a^{\wedge}}{\rightleftharpoons}} \mathbf{CB}^{\wedge} \underset{[H^+]}{\overset{K_a^{\wedge\wedge}}{\rightleftharpoons}} \mathbf{CB}^{\wedge -} \underset{[H^+]}{\overset{K_a^{\wedge\wedge\wedge}}{\rightleftharpoons}} \mathbf{CB}^{\wedge 2-} \quad (19)$$

$$\chi_{\mathbf{AH}^+} = \frac{[H^+]^3}{D};\ \chi_{\mathbf{CB}^{\wedge}} = \frac{K_a^{\wedge}[H^+]^2}{D};\ \chi_{\mathbf{CB}^{\wedge -}} = \frac{K_a^{\wedge}K_a^{\wedge\wedge}[H^+]}{D};\ \chi_{\mathbf{CB}^{\wedge 2-}} = \frac{K_a^{\wedge}K_a^{\wedge\wedge}K_a^{\wedge\wedge\wedge}}{D} \quad (20)$$

with

$$D = [H^+]^3 + K_a^{\wedge}[H^+]^2 + K_a^{\wedge}K_a^{\wedge\wedge}[H^+] + K_a^{\wedge}K_a^{\wedge\wedge}K_a^{\wedge\wedge\wedge} \quad (21)$$

In Figure 4c, the mole fraction of $\mathbf{CB}^{\wedge}$, eq 19, is decomposed into its **A**, **B**, and **Cc** components, respectively, by the fitting coefficients a_0, b_0, and c_0 ($a_0 + b_0 + c_0 = 1$) and identically for the anionic forms of $\mathbf{CB}^{\wedge}$, eqs 22 to 24.

$$\chi_{\mathbf{AH}^+} + \chi_{\mathbf{A}} = \frac{[H^+]^3 + a_0 K_a^{\wedge}[H^+]^2}{D} \quad (22)$$

https://doi.org/10.1021/acsomega.1c04456
ACS Omega 2021, 6, 30172−30188

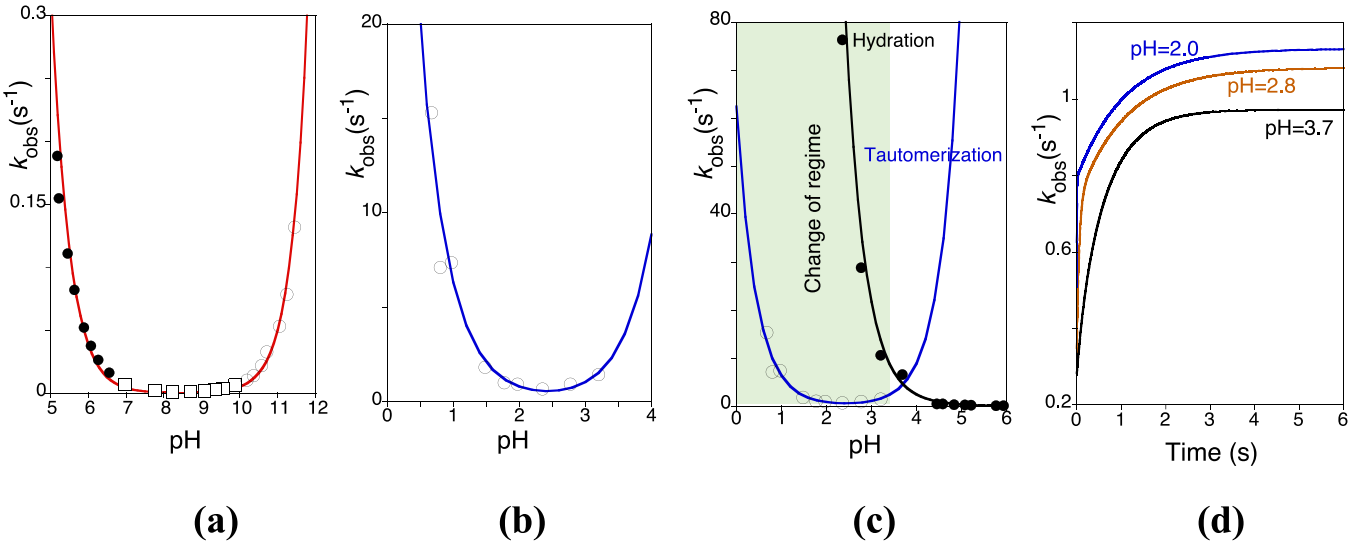

Figure 5. (a) Rate constants for the faster process after reverse pH jumps: (solid circles) monitored by stopped flow from pH = 7 back to lower values; (open squares) direct pH jumps monitored by a standard spectrophotometer; (open circles) direct pH jumps to the basic region followed by stopped flow. Fitting was achieved by means of eq 16 where $k_h = 0.3\ s^{-1}$ and $k_{-h} = 2.1 \times 10^4\ M^{-1}\ s^{-1}$ for the acidic region and eq 18 for the basic region where $k_{OH} = 50\ M^{-1}\ s^{-1}$; (b) the same as (a) for the slower step. Fitting was achieved with eq 17 for $k_{-t} = 0.084\ s^{-1}$, $k_{-t}^{H} = 62\ M^{-1}\ s^{-1}$, and $k_{-t}^{OH} = 8.9 \times 10^{10} M^{-1}\ s^{-1}$; (c) representation of the pH dependence of the hydration and tautomerization rates; (d) traces of the reverse pH jumps at different final pH values. At pH > 3.7, tautomerization becomes much faster than hydration.

Table 1. Equilibrium Constants of the Compound 4′-Hydroxyflavylium at 60 °C, Obtained by Reverse pH Jumps Monitored by Stopped Flow[24]

pK_a	pK_h	K_t	$pK^{\wedge}_a$	$pK^{\wedge\wedge}_a$	$pK^{\wedge\wedge\wedge}_a$	pK_{B/B^-}	pK_{Cc/Cc^-}	$pK_{Cc^-/Cc^{2-}}$
4.85	4.86	0.88	4.4	8.6	9.5	8.95	8.1	9.5

$$\chi_B + \chi_{B^-} + \chi_{B^{2-}} = \frac{b_0 K_a^{\wedge}[H^+]^2 + b_1 K_a^{\wedge} K_a^{\wedge\wedge}[H^+] + b_2 K_a^{\wedge} K_a^{\wedge\wedge} K_a^{\wedge\wedge\wedge}}{D} \quad (23)$$

$$\chi_{Cc} + \chi_{Cc^-} + \chi_{Cc^{2-}} = \frac{c_0 K_a^{\wedge}[H^+]^2 + c_1 K_a^{\wedge} K_a^{\wedge\wedge}[H^+] + c_2 K_a^{\wedge} K_a^{\wedge\wedge} K_a^{\wedge\wedge\wedge}}{D} \quad (24)$$

The parameters *a*, *b*, and *c* are obtained by fitting as in Figure 4c. It is straightforward to prove that they permit the calculation of all equilibrium constants of the pseudo-equilibrium.[24]

$$K_a = a_0 K_a^{\wedge};$$
$$K_h = b_0 K_a^{\wedge};$$
$$K_{B/B^-} K_h = b_1 K_a^{\wedge} K_a^{\wedge\wedge};$$
$$K_{B^-/B^{2-}} K_{B/B^-} K_h = b_2 K_a^{\wedge} K_a^{\wedge\wedge} K_a^{\wedge\wedge\wedge};$$
$$K_h K_t = c_0 K_a^{\wedge};$$
$$K_{Cc/Cc^-} K_h K_t = c_1 K_a^{\wedge} K_a^{\wedge\wedge};$$
$$K_{Cc^-/Cc^{2-}} K_{Cc/Cc^-} K_h K_t = c_2 K_a^{\wedge} K_a^{\wedge\wedge} K_a^{\wedge\wedge\wedge} \quad (25)$$

In Table 1, the equilibrium constants of 4′-hydroxyflavylium are reported. Regarding the rate constants, it is now possible to calculate $k_h = 0.3\ s^{-1}$ and $k_{-h} = 2.1 \times 10^4\ M^{-1}\ s^{-1}$, from the rates of the second step (eq 16 and Figure 5a).

2.3. Toward Equilibrium. In the case of the compound 4′-hydroxyflavylium, the rates to attain equilibrium were extremely slow, and the experiments were carried out at 60 °C (Figure 6).

In Figure 6a, a direct pH jump from pH = 1 to pH = 5.1 is shown. The spectral variations indicate that basically all quinoidal base disappears to give *trans*-chalcones (**Ct**, **Ct**$^-$, and **Ct**$^{2-}$ according to the final pH). The same is observed for higher pH values. In Figure 6b, the individual spectra of the *trans*-chalcones obtained from the titration of **Ct**$^{2-}$ ($pK'_a = 3.9$, $pK_{Ct/Ct^-} = 7.86$, and $pK_{Ct^-/Ct^{2-}} = 8.95$) by mathematical decomposition are shown, and the mole fraction distribution of the equilibrium species is presented in Figure 6c.

In conclusion, at equilibrium, eq 26, the flavylium cation behaves as a triprotic acid, and the **CB** species for this particular system are *trans*-chalcones.

$$\mathbf{AH^+} \underset{[H^+]}{\overset{K'_a}{\rightleftharpoons}} \mathbf{CB} \underset{[H^+]}{\overset{K''_a}{\rightleftharpoons}} \mathbf{CB^-} \underset{[H^+]}{\overset{K'''_a}{\rightleftharpoons}} \mathbf{CB^{2-}} \quad (26)$$

3. EXAMPLES OF MOLECULAR METAMORPHOSIS SYSTEMS

3.1. Introducing the Flavanone in the Metamorphic System. The number, nature, and position of the substituents can modulate the metamorphic systems generated by flavylium cations. It is the case of those possessing a hydroxyl substituent in position 2′, see Scheme 7, because a flavanone is introduced in the metamorphic system.[27−30]

Contrary to the behavior of anthocyanins and related compounds in the case of 5′-methyl-2′-hydroxyflavylium, the disappearance rate of the quinoidal base does not drop to very small values, and a plateau is reached around neutrality with k_{obs}

https://doi.org/10.1021/acsomega.1c04456
ACS Omega 2021, 6, 30172−30188

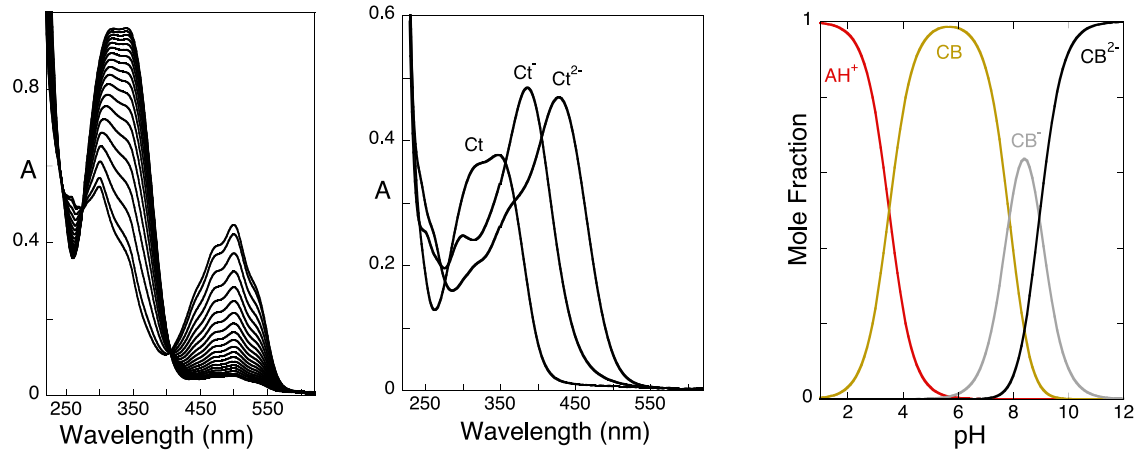

Figure 6. (a) Direct pH jump of 4′-hydroxyflavylium from pH = 1 to pH = 5.1 at 60 °C. The system follows a monoexponential function with a rate constant of 9×10^{-4} s^{-1}; (b) individual spectra of the *trans*-chalcones obtained from the titration of $\mathbf{Ct}^{2-}$, ($pK_{AH^+/Ct} = 3.9$; $pK_{Ct/Ct^-} = 7.86$; $pK_{Ct^-/Ct^{2-}} = 8.95$) by mathematical decomposition; (c) mole fraction distribution of the multistate species at equilibrium. The species **CB**, $\mathbf{CB}^-$, and $\mathbf{CB}^{2-}$ correspond to the **Ct**, $\mathbf{Ct}^-$, and $\mathbf{Ct}^{2-}$.

= 1 s^{-1}.[27] Consequently, after a few seconds, this kinetic step is finished, and the pseudo-equilibrium is attained corresponding to the initial spectrum of Figure 7a. Considering that the $pK^{\wedge}_a$ and $pK^{\wedge\wedge}_a$ of this system are 3.5 and 7.5, a direct pH jump to 6.1 is constituted essentially by the anionic species $\mathbf{B}^-$ and $\mathbf{Cc}^-$. The increase in the absorbance in Figure 7a is due to the formation of the $\mathbf{Ct}^-$ species. At this point, it is a common behavior of most of the synthetic flavylium compounds like 4′-hydroxyflavylium, 7′-hydroxyflavylium, and 4′,7-dihydroxyflavylium among many others, where in a basic medium, the stable species are anionic *trans*-chalcones. The novelty of this system is the spectral variation of Figure 7b, indicating that in this case, the anionic *trans*-chalcone gives the flavanone. This observation was corroborated by ^{1}H NMR experiments.[27]

Scheme 7. Flavylium−Flavanone System

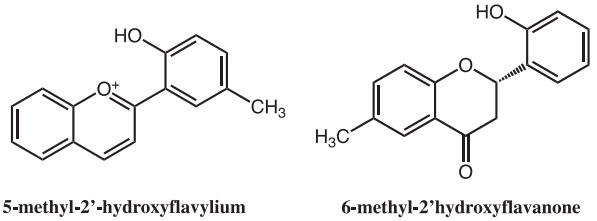

5-methyl-2'-hydroxyflavylium 6-methyl-2'hydroxyflavanone

3.1.1. Illustrating the Concept of a Timer at the Molecular Level. The system generated by 5′-methyl-2′-hydroxyflavylium was used to illustrate the concept of a timer at the molecular level (Scheme 8).

The molecular metamorphosis cycle starts with **Ct**. The **Ct** is stable at pH = 4 and could be prepared from the generator flavylium cation in a slow process or very fast after a pH jump to pH = 13 that gives $\mathbf{Ct}^{2-}$ followed by adjusting the pH to 4. The timer is activated by a direct pH jump to pH = 8 forming $\mathbf{Ct}^-$, which triggers the formation of the flavanone as shown in Figure 6b. The timer can be stopped (lock step) by a pH jump back to pH = 4. The fraction of $\mathbf{Ct}^-$ that did not react is transformed into the stable **Ct**. The flavanone (FLV) is stable unless at higher pH values, see below. The ratio **Ct**/FLV can be measured (read the timer) from the disappearance of **Ct**, and the ratio **Ct**/FLV is more or less linear up to 200 min (Figure 6c), the time interval for the use of the timer. The unlock step is achieved through a pH jump from pH = 4 to pH = 13. At this pH, **Ct** is transformed into $\mathbf{Ct}^{2-}$, and the flavanone deprotonates and in a fast process gives $\mathbf{Ct}^{2-}$. The system could be prepared for a next cycle by the reset step, a pH jump from pH = 13 to pH = 4.

3.2. Response of the Flavylium-Based Metamorphosis to Light Inputs, the Write-Lock-Read-Unlock-Erase Molecular Switching System. Molecular species presenting two forms whose interconversion can be modulated by external stimuli are directly linked to the chemistry of signal generation, transfer, conversion storage, and detection.[1,31−34] In this frame, flavylium-based photochromic systems capable of write-lock-read-unlock-erase have been reported.[6]

The concept of the optical memory is illustrated in Scheme 9 for the compound 4′-methoxyflavylium,[6] which at equilibrium at pH 6 is basically constituted by **Ct**. This compound in particular exhibits an extremely high *cis*−*trans* isomerization barrier. The light input writes information through the *trans* to *cis* isomerization. The pseudo-equilibrium at pH = 6 is reached in subseconds. The high isomerization barrier prevents the auto-erasing of information. However, it is not convenient to read information at this stage because the light absorption by **Cc** gives rise to the formation of **Ct**, erasing the signal. The lock step consists of a reverse pH jump to pH = 1 that leads to the appearance of the flavylium cation. This species is not photochromic, and information can be read. To cancel information for a next cycle, it is necessary to unlock the system by direct pH jumps to pH = 6, in other words, to the pseudo-equilibrium at pH = 6. The unlock step should be followed by the erasing step using light or by heating the system to overcome the isomerization barrier.

3.3. One-Way Cycle of Direct−Reverse pH Jumps. The one-way cycle generated by the flavylium cation is shown in Scheme 10. After a direct pH jump, quinoidal bases are formed and disappear leading to the equilibrium (or the pseudo-

https://doi.org/10.1021/acsomega.1c04456
ACS Omega 2021, 6, 30172−30188

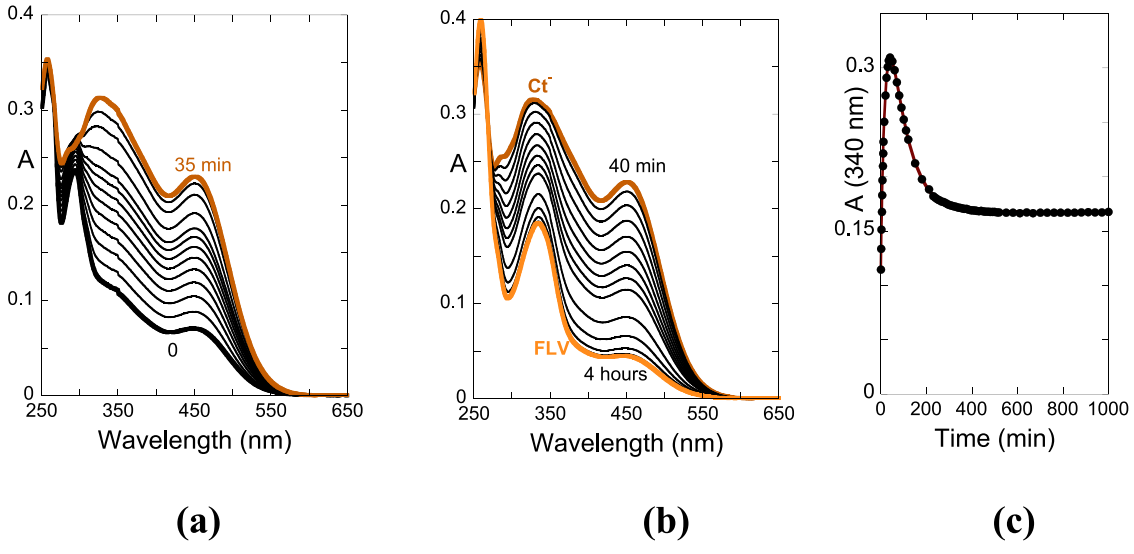

Figure 7. (a) Spectral variations after a direct pH jump from the 5′-methyl-2′-hydroxyflavylium cation at pH = 1 to pH = 8.1. The spectrum at $t = 0$ is basically constituted by anionic species $\mathbf{B}^-$ and $\mathbf{Cc}^-$, ($pK^{\wedge}_a = 3.5$ and $pK^{\wedge\wedge}_a = 7.5$); (b) evolution of the absorption spectra of the same pH jump after 40 min until reaching equilibrium, essentially constituted by flavanone; (c) trace at 340 nm to evidence both steps. Adapted with permission from ref 27. Copyright 2018. Elsevier.

Scheme 8. Illustrating the Concept of a Timer at the Molecular Level by Means of the Metamorphosis Cycle Generated by 5′-Methyl-2′-hydroxyflavylium.

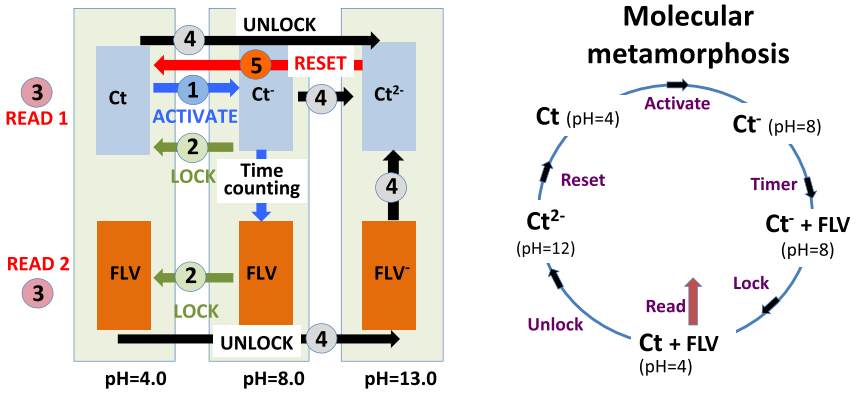

Adapted with Permission from Ref 27. Copyright 2018. Elsevier

Scheme 9. Illustrating the Concept of an Optical Memory Based on a Molecular Metamorphosis Cycle

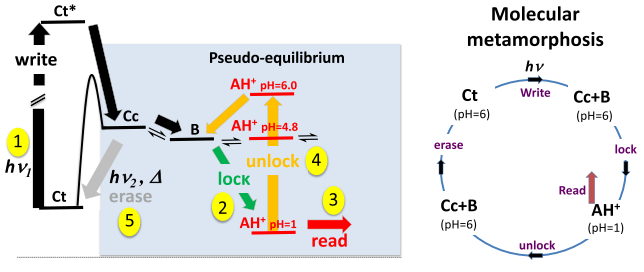

Scheme 10. One-Way Cycle Obtained by a Succession of Direct pH Jumps from the Generator Molecule Followed by Reverse pH Jumps back to pH = 1

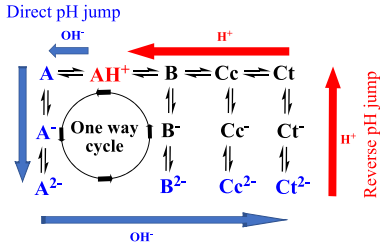

equilibrium). A reverse pH jump restores the species of the first row, which evolve to the flavylium cation at different rates without forming the quinoidal base. This unidirectional cycle is only possible when the direct pH jump is performed to basic pH values where the quinoidal bases are hydrated by OH^-. At acidic/neutral conditions, the quinoidal bases are stable and can only be consumed through the hydration of the flavylium cation.

3.4. Interconversion of the Flavylium Cation with 2,2′-Spirobis[chromene] Derivatives. One class of styrylflavylium compounds yields chalcones capable of closing at both sides following a reverse pH jump to give flavylium cations (via **Cc** and **B**), as shown in Scheme 11.[2,35−37] When the *trans*-chalcone is symmetric, the closure of the ring leads to the same flavylium cation, independent of the side on which the reaction takes place. However, if the *trans*-chalcone is asymmetric, then

https://doi.org/10.1021/acsomega.1c04456
ACS Omega 2021, 6, 30172−30188

Scheme 11. Metamorphosis in 2′-Hydroxystyrylflavylium[a]

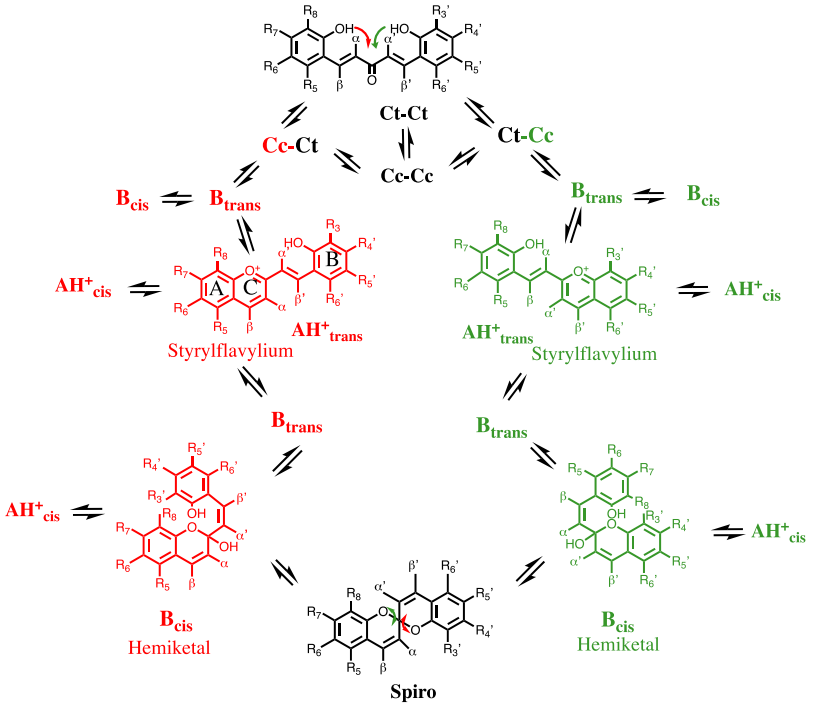

Adapted with permission from ref 36. Copyright 2020. Elsevier. [a]The common *trans*-chalcone can close the ring upon a reverse pH jump through two routes, as indicated in green and red. For symmetric *trans*-chalcones, the two routes are the same, but for asymmetric *trans*-chalcones, two different flavylium isomers are obtained.[2] The numeration was chosen to maintain coherence with that of the flavylium cation. Interconversion can also be achieved through the spiro species.

two isomers of the flavylium cation can be formed. In addition to the formation of different flavylium cation isomers, the formation of a spiro compound, as shown in Scheme 11, was reported.[2,38] The isomerization between the two flavylium compounds can take place from the common *trans*-chalcone or through the spiro compound.

The interconversion between 2-(2,4-dihydroxystyryl)-1-benzopyrylium chloride and 7-hydroxy-2-(2-hydroxystyryl)-1-benzopyrylium chloride in water/ethanol (80:20) at pH = 1.68 was monitored by UV−vis and ^{1}H NMR experiments, as shown in Figure 8.[2] These data clearly indicate that the initial compound resulting from the synthesis of 2-(2,4-dihydroxystyryl)-1-benzopyrylium (**AH**$^+$) was slowly converted through a first-order kinetic process, with a rate constant of 2.5×10^{-5} s^{-1}, into 7-hydroxy-2-(2-hydroxystyryl)-1-benzopyrylium (**AH**$^+_{iso}$), to reach an equilibrium between the two flavylium compounds (58% **AH**$^+$ + 42% **AH**$^+_{iso}$).

To explain the details of the kinetic behavior, the formation of a spiro transient was postulated. Although no spectral evidence was achieved at the time, the interconversion between spiro and 2-(2-hydroxystyryl)-1-benzopyrylium compounds was first reported by Decker and Felser in 1908.[2,39]

The formation of the spiro was directly observed in a similar family of compounds, in which rings **C** and **B** of the flavylium cation are linked by a cyclohexane bridge, as shown in Scheme 12.[36] The species synthesized under this study was a **Ct**$_{trans}$ 2,6-bis(2-hydroxybenzylidene)cyclohexanone. After a reverse pH jump from the **Ct**$_{trans}$ species to moderately acidic solutions, the color fades and hailing crystals suitable for single-crystal X-ray analysis are formed. The structure showed that this product was the respective spiro, as shown at the top of Scheme 12.

The spiro is stable in moderately acidic solutions. Under very acidic conditions, at $[H_3O^+]$ = 2 M, the spiro is rapidly converted into the flavylium cation, and in basic solutions, it gives anionic chalcones, which can restore the neutral chalcone by adjusting the pH around neutrality. The kinetic process is presented at the bottom of Scheme 12.

More recently, from the multistate of 2,6-bis(5-bromo-2-hydroxybenzylidene)cyclohexanone, single-crystal structures of the respective flavylium cation and spiro were reported by Cseh et al.[40]

The asymmetric **Ct**$_{trans}$ 2,6-bis(arylidene) cyclohexanone shown in Scheme 13 is the parent of the **Ct**$_{trans}$ shown in Figure 8 but with the cyclohexane bridge.[41] In this case, only the crystal structure of the flavylium cation was obtained. The spiro was isolated and identified by ^{1}H NMR and by its characteristic UV−vis absorption spectra. Unlike the parent compound, which lacks the cyclohexane bridge, no isomerization corresponding to the migration of the hydroxyl from position 7 to position 2′ of the flavylium cation was observed (Scheme 13b). This finding indicates that at least under the given experimental conditions, the closure of the *trans*-chalcone and the opening of the spiro give the same flavylium isomer.

The symmetric spiro shown in Scheme 14 was also characterized from the synthesis of (4-(2,4-dihydroxybenzylidene)-6-hydroxy-1,2,3,4-tetrahydroxanthylium chloride) compound I. In this case, the opening of the spiro and the closure of the respective *trans*-chalcone (via **Cc** and **B**) lead necessarily to the same flavylium cation.[42]

Another metamorphic system based on a symmetric spiro compound was identified in (*E*)-6-(dimethylamino)-4-(4-(dimethylamino)-2-hydroxybenzylidene)-1,2,3,4-tetrahydroxanthylium chloride, as shown in Scheme 15.[43]

https://doi.org/10.1021/acsomega.1c04456
ACS Omega 2021, 6, 30172−30188

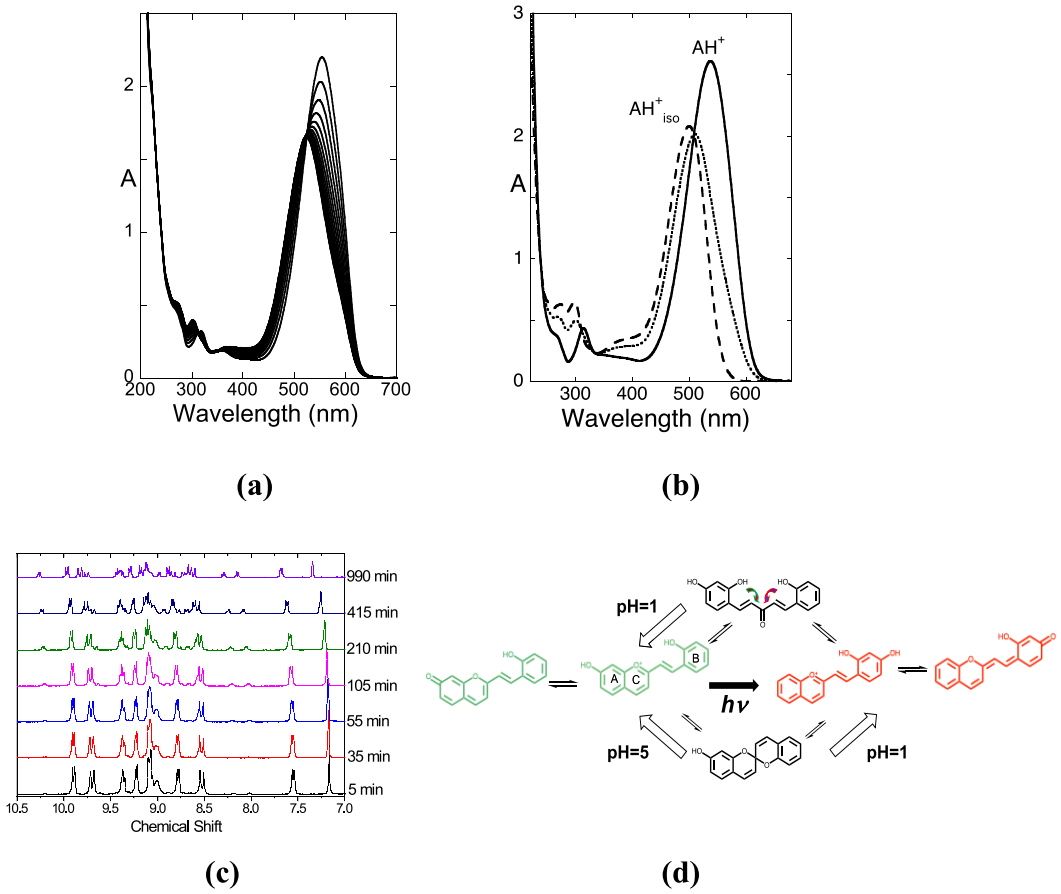

Figure 8. (a) Spectral variations observed upon the dissolution of 2-(2,4-dihydroxystyryl)-1-benzopyrylium chloride in water/ethanol (80:20) at pH = 1.68; (inset) absorbance variation at 537 nm as a function of the reaction time; (b) spectra of the initial compound (solid line), of the equilibrated mixture (dotted line), and of the product (dashed line), 7-hydroxy-2-(2-hydroxystyryl)-1-benzopyrylium, which was obtained by the mathematical decomposition of the spectrum of the stationary state; (c) ^{1}H NMR spectra of 2-(2,4-dihydroxystyryl)-1-benzopyrylium chloride in D_2O/CD_3OD (80:20) at pD = 1.87 as a function of time; (d) spiro proposed as an intermediate in the conversion of the two isomers. Adapted with permission from ref 2. Copyright 2012. American Chemical Society.

The direct pH jumps from the flavylium cation initially give a pseudo-equilibrium, as shown in Scheme 15 (orange traced lines), involving protonated and nonprotonated flavylium cations and a quinoidal base, which is the species at pH > 9. At equilibrium (dark traced lines) in moderately basic solutions, a fraction of the quinoidal base disappears to give the spiro. No neutral *trans*-chalcone was observed, but its anionic form was detected at much higher pH values. At pH = 10, the spiro is in equilibrium with the quinoidal base. After a reverse pH jump, the quinoidal base is transformed into the flavylium cation or its protonated form (depending on pH), and it is possible to follow the kinetics of the spiro ring opening as a function of the pH. From the pH dependence of this reaction, there is evidence of the involvement of the protonated spiro form at lower pH values.

The relation between the colorless spiro and some colored species of the corresponding styrylflavylium multistate has many possibilities to explore. The spiro is a type of reservoir that could produce color following external stimuli, such as pH and light. This property opens up many possibilities toward creating practical applications, from photochromic systems to models for optical memory and others, through the ingenuity of chemists.

3.5. 6,8 A-Ring Substituent Rearrangements. Another interesting example of chemical metamorphosis based on the flavylium multistate can be observed for flavylium cation generators bearing a hydroxyl substituent in position 5 and comprising different substituents in positions 8 and 6.

To the best of our knowledge, the early 6,8 A-ring substituent rearrangement was reported by Jurd,[44,45] who observed that 5,7,8,4′-tetrahydroxyflavylium is quantitatively converted into the corresponding 5,7,6,4′-tetrahydroxyflavylium isomer upon dissolution in acidic aqueous solutions (Scheme 16).[44−46]

The rate of the rearrangement reaction was found to be pH-dependent, and it proceeded much more rapidly under less acidic conditions. At pH 2.6, equilibrium is achieved in approximately 7 h, while in a 1% HCl solution, the reaction takes 3 days. This process was also confirmed to be strongly dependent on temperature, decreasing from 3 days to 30 min with warming. Although this early work lacks important experimental details and quantitative data (such as rate constants, temperatures, etc.), it provided the first evidence of the 6,8 rearrangement through the reversible ring-opening reaction characteristic of the flavylium multistate.

As mentioned above, the *sine qua non* to observe the 6,8 A-ring substituent rearrangement is the existence of different substituents in positions 6 and 8; otherwise, the same isomer is formed as in 3-deoxyanthocyanins, such as luteolinidin.

A systematic study on the 6,8 rearrangements of the flavylium cation of *C*-glycosyl-3-deoxyanthocyanidins in acidic aqueous solutions was published by Andersen et al.[47] Contrary to the

https://doi.org/10.1021/acsomega.1c04456
ACS Omega 2021, 6, 30172−30188

Scheme 12. Top: Crystal Structure of the Spiro;[36] Bottom: Kinetic Scheme of the Metamorphosis System Generated by 2,6-Bis(2-hydroxybenzylidene)cyclohexanone.

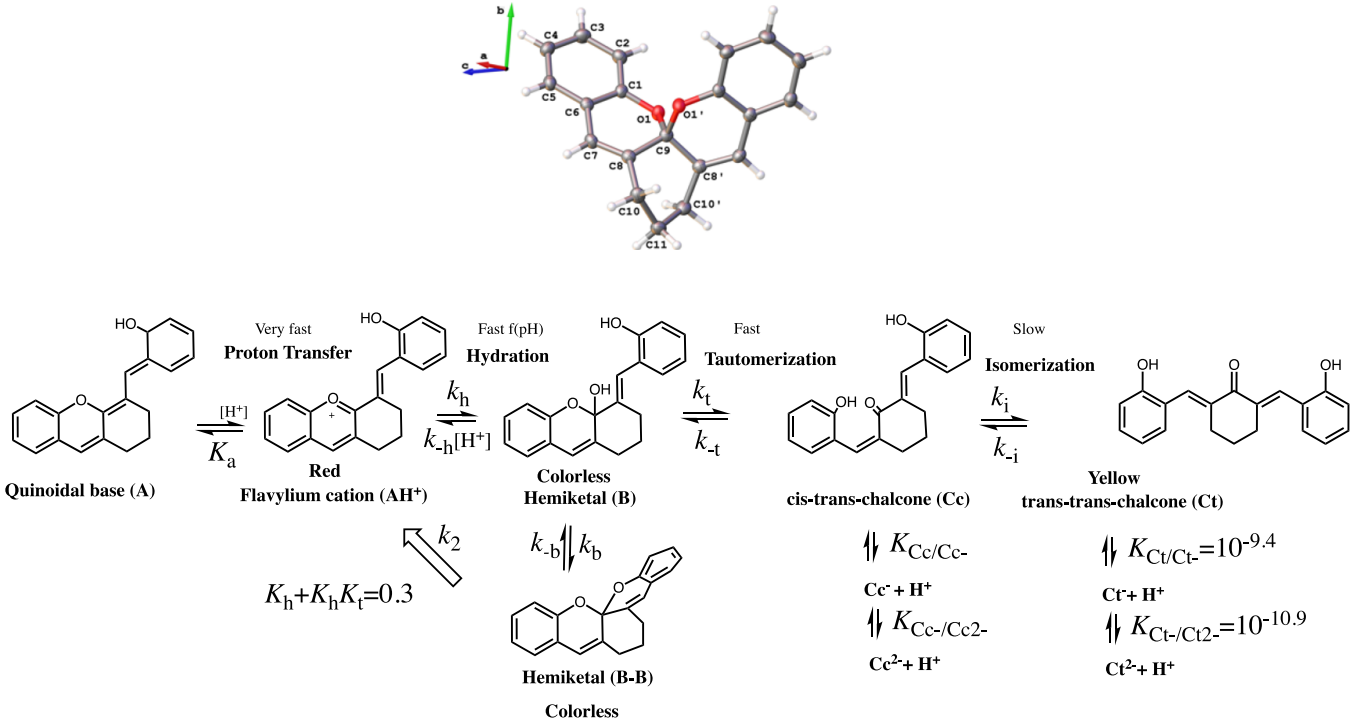

Reproduced with Permission from Ref 36. Copyright 2014. American Chemical Society

Scheme 13. (a) General Kinetic Scheme Based on the Asymmetric Chalcone (2*E*,6*E*)-2-(2,4-Dihydroxybenzylidene)-6-(2-hydroxybenzylidene)cyclohexanone; (b) Unlike the Parent Compound, Which Lacks the Cyclohexane Bridge, No Isomerization Corresponding to the Migration of the Hydroxyl from Position 7 to Position 2′ of the Flavylium Cation Was Observed

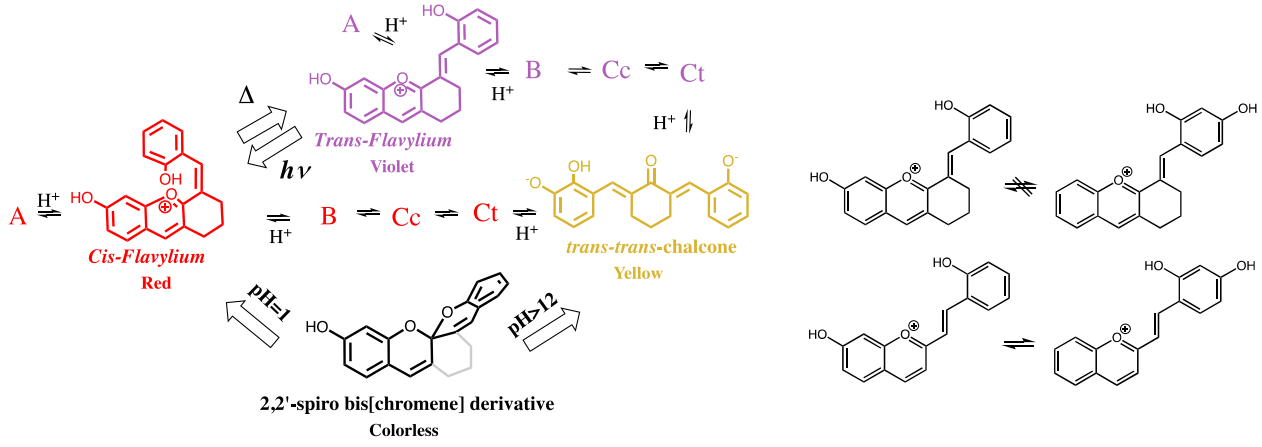

Scheme 14. Symmetric Spiro (II) Obtained from the Flavylium Cation (I)

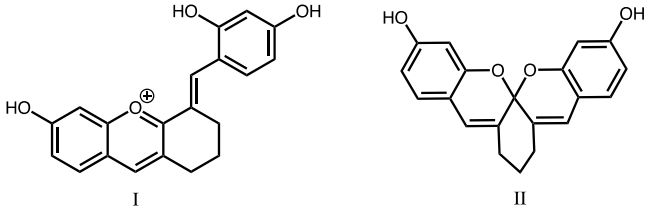

findings of Jurd, who observed quantitative conversion, these authors verified that whether starting with pure 6-*C*- or pure 8-*C*-glycosyl-3-deoxyanthocyanidin, an equilibrium between these two forms is reached. Isolating pure isomers by HPLC-DAD allowed the researchers to observe that the UV−vis absorption spectra of the 8-*C*-glycosyl-3-deoxyanthocyanidin isomers are redshifted with respect to those of their 6-*C*-glycosyl-3-deoxyanthocyanidin counterparts, a feature that was also reported for 5,7,8,4′-tetrahydroxyflavylium/5,7,6,4′-tetrahydroxyflavylium by Jurd.

https://doi.org/10.1021/acsomega.1c04456
ACS Omega 2021, 6, 30172−30188

Scheme 15. Metamorphic System Based on a Styrylflavylium Bearing the Cyclohexane Bridge and Diethylamine Substituents.

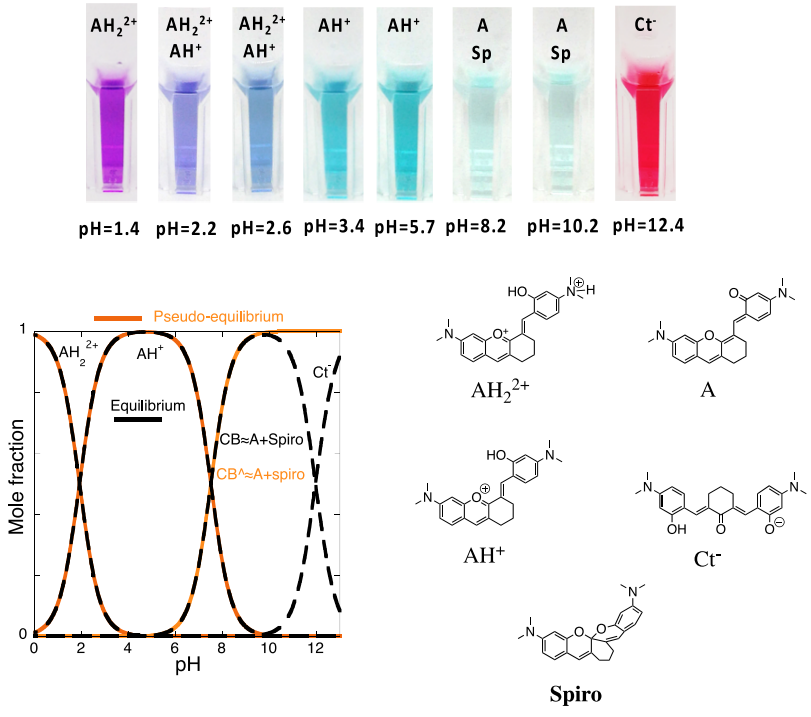

Adapted with Permission from Ref 43. Copyright 2018. American Chemical Society

Scheme 16. Isomeric Rearrangement in 5,7,8,4′-Tetrahydroxyflavylium (Aurantinidin)

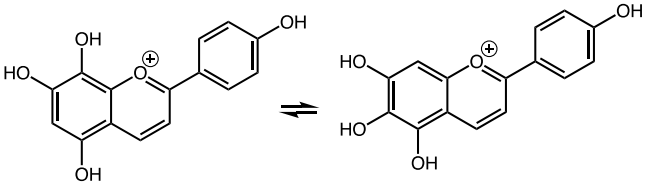

The study of the 6,8 rearrangement was extended to higher pH values.[48,49] The multistate of species that appear in an acidic to neutral medium is presented in Scheme 17. Scheme 17 shows that the theoretical possibilities of communication between the two systems can only be performed, as expected, through neutral or anionic *cis*- and *trans*-chalcones.

An example of this type of multistate was reported for 6-bromo-apigeninidin (**6-Br**) and 8-bromo-apigeninidin (**8-Br**).[48] Despite its complexity, the system can be treated as a single polyprotic acid. In fact, the UV−vis pH-dependent spectral

Scheme 17. Multistate of Species in a 6,8 Rearrangement Including Neutral and Anionic Forms[a]

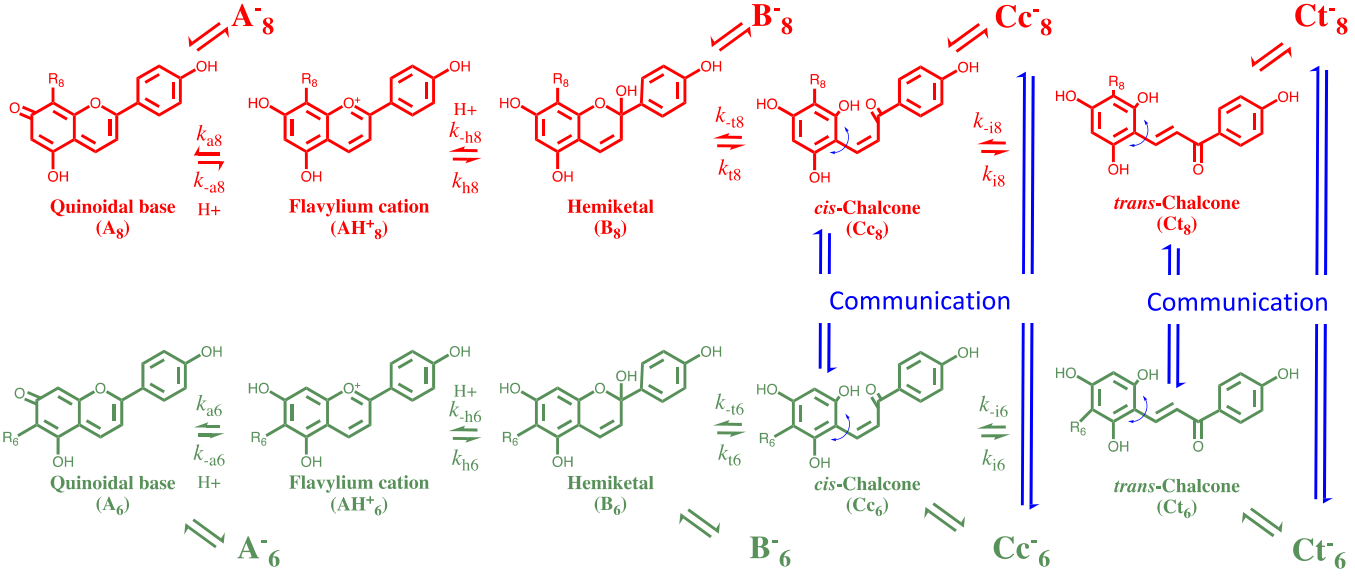

[a]The theoretical possibilities of communication between the two multistates are indicated in blue.

https://doi.org/10.1021/acsomega.1c04456
ACS Omega 2021, 6, 30172−30188

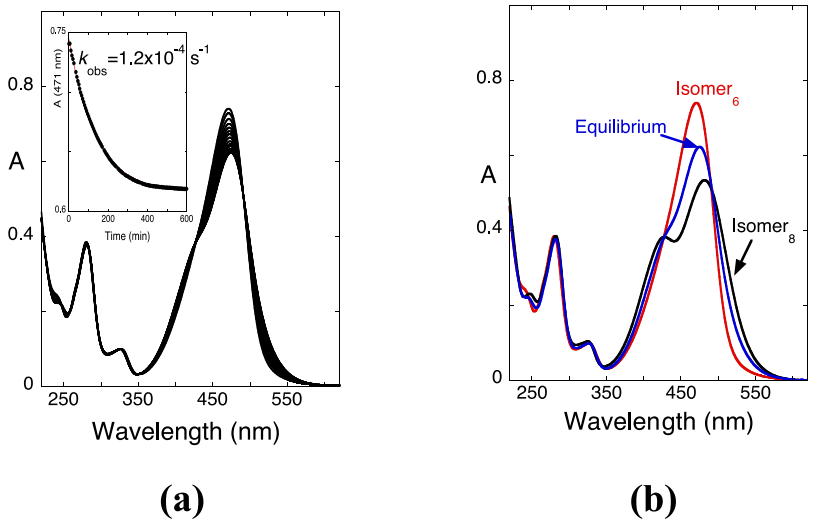

Figure 9. (a) Spectral variations of **6-Br** (7×10^{-5} M) upon separation by HPLC, pH 1.0, in water/EtOH (4:1, v:v). (inset) Absorbance variations at 471 nm as a function of time showing pseudo-first-order kinetics fitted with $k_{obs} = 1.2 \times 10^{-4}$ s^{-1}. (b) Absorption spectra of both isomers (7×10^{-5} M). The equilibrium is a mixture of 52% isomer 8 and 48% isomer 6, as estimated by spectral decomposition. Adapted with permission from ref 48. Copyright 2016. ChemPubSoc Europe.

Scheme 18. The Metamorphosis Cycle of the 6,8 Rearrangement (6-Br and 8-Br) Operated with Host–Guest Inputs.

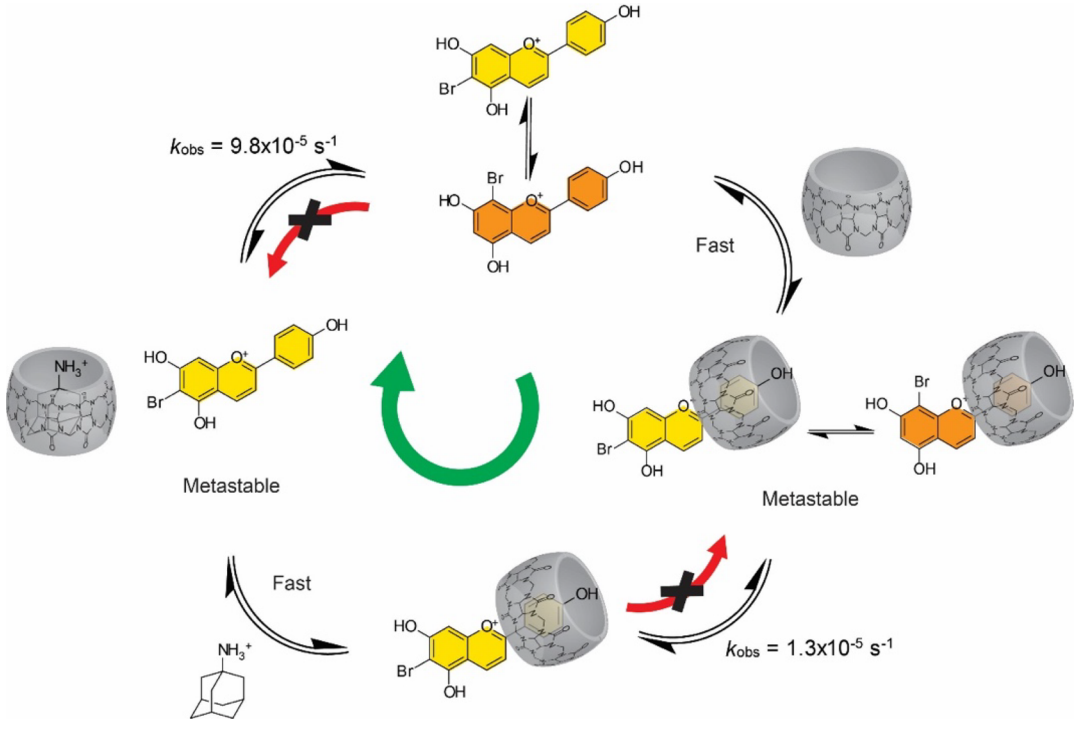

Adapted with Permission from Ref 50. Copyright 2016. American Chemical Society

variations in an acidic medium are compatible with a diprotic acid with pK_as of 2.55 and 5.4.[48]

The two flavylium cation isomers were separated by HPLC. The evolution of the absorption spectra for **6-Br** at pH = 1.0 is shown in Figure 9a. This compound presented similar mole fractions of the 6 and 8 isomers in equilibrium, supporting previous reports indicating that the nature and position of the substituents may affect the equilibrium composition.[47]

The thermodynamics and kinetics of the 6,8 rearrangement can be dramatically modified by host–guest interactions.[49,50] Upon the addition of cucurbit[7]uril (CB7) to an equilibrated solution containing both isomers at pH = 1, the system evolves a new equilibrium that is reached in 3 days at 25 °C but can be sufficiently accelerated to 1 h by warming the solution at 70 °C without affecting the final composition significantly.[50] Using UV–vis and ^{1}H NMR experiments, the new equilibrium was demonstrated to be exclusively composed of a host–guest complex formed between **6-Br** and CB7. This amplification phenomenon was attributed to the exceptional selectivity of CB7 for **6-Br** over **8-Br**, probably due to the repulsive interactions established between the carbonyl portals of the host and the Br substituent in position 8. Host–guest titration

https://doi.org/10.1021/acsomega.1c04456
ACS Omega 2021, 6, 30172–30188

experiments afforded binding constants of $K = 2.5 \times 10^5$ M^{-1} for **6-Br** and $K = 5 \times 10^3$ M^{-1} for **8-Br**, consistent with the observed selectivity.

The observed amplification of the 6-bromo isomers from the 1:1 mixture allowed for the conception of a metamorphosis molecular cycle with host−guest inputs (Scheme 18). Adding CB7 to an equilibrated solution containing a mixture of isomers leads to the formation of a metastable state containing a mixture of host−guest complexes. This mixture evolves with a $k_{obs} = 1.3 \times 10^{-5}$ s^{-1} to the single **6-Br**/CB7 complex owing to its higher relative stability. At this point, the system cannot be microscopically reverted to the mixture of complexes. However, 1-aminoadamantane (AD) forms ultrastable host−guest complexes with CB7 ($K = 4 \times 10^{12}$ M^{-1})[51] and can be used to release the isomer **6-Br** from the CB7 cavity efficiently through competitive binding. This step originates free **6-Br** in a metastable state and evolves to the initial 50:50 mixtures of free isomers, with $k_{obs} = 9.8 \times 10^{-5}$ s^{-1} closing the cycle. The reversible interconversion between the two thermodynamically stable states, *i.e.*, the mixture of free isomers and the amplified **6-Br**/CB7 complex, occurs through different microscopic pathways and therefore imposes directionality on the cycle.

4. CONCLUSIONS

Flavylium compounds are prime examples of systems capable of chemical metamorphosis. These apparently simple molecules, often represented as flavylium salts, can generate complex reaction networks comprising several species in equilibrium with interconversion rates that span over timescales that range from microseconds to months. Furthermore, when functionalized with specific functional groups in particular positions, flavylium cations can generate other flavylium isomers with different chemical and physical properties, which increase the number of species in the reaction network and expand the complexity of conventional compounds.

The reversible nature of the chemical transformations comprising the reaction network of flavylium compounds allows for their potential applications in molecular devices such as optical memories, logic gates, and molecular timers. However, these systems have been mostly explored as diluted isolated molecules in solution, soft materials, or microheterogeneous media. We envisage that the incorporation of these molecules in polymers, nanoparticles, surfaces, interfaces, and as molecular building blocks to construct molecular machines and complex supramolecular systems may lead to the development of new materials with complex responsive and adaptive properties.

AUTHOR INFORMATION

Corresponding Author

Fernando Pina − *LAQV−REQUIMTE, Departamento de Química, Faculdade de Ciências e Tecnologia, Universidade Nova de Lisboa, Caparica 2829-516, Portugal;* orcid.org/0000-0001-8529-6848; Email: fp@fct.unl.pt

Authors

Nuno Basílio − *LAQV−REQUIMTE, Departamento de Química, Faculdade de Ciências e Tecnologia, Universidade Nova de Lisboa, Caparica 2829-516, Portugal;* orcid.org/0000-0002-0121-3695

A. Jorge Parola − *LAQV−REQUIMTE, Departamento de Química, Faculdade de Ciências e Tecnologia, Universidade Nova de Lisboa, Caparica 2829-516, Portugal;* orcid.org/0000-0002-1333-9076

Diogo Sousa − *IBB-Institute for Bioengineering and Biosciences, Instituto Superior Técnico, Universidade de Lisboa, Lisbon 1049-003, Portugal*

Vesselin Petrov − *Physical Chemistry Department, Faculty of Chemistry and Pharmacy, University of Sofia, Sofia 1504, Bulgaria;* orcid.org/0000-0003-4503-4602

Luis Cruz − *LAQV−REQUIMTE, Departamento de Química e Bioquímica, Faculdade de Ciências, Universidade do Porto, Porto 4169-007, Portugal;* orcid.org/0000-0003-2226-0404

Victor de Freitas − *LAQV−REQUIMTE, Departamento de Química e Bioquímica, Faculdade de Ciências, Universidade do Porto, Porto 4169-007, Portugal;* orcid.org/0000-0003-0586-2278

Complete contact information is available at: https://pubs.acs.org/10.1021/acsomega.1c04456

Notes

The authors declare no competing financial interest.

ACKNOWLEDGMENTS

This work was supported by the Associated Laboratory for Sustainable Chemistry, Clean Processes and Technologies LAQV through the national funds from UIDB/50006/2020 and UIDP/50006/2020 as well as the European Regional Development Fund within the Operational Programme "Science and Education for Smart Growth 2014−2020" under the Project CoE "National Center of Mechatronics and Clean Technologies" (BG05M2OP001-1.001-0008). N.B. is grateful to FCT for the contract CEECIND/00466/2017, D.S. for the doctoral grant (SFRH/BD/143369/2019), and L.C. for the research contract DL 57/2016/CP1334/CT0008.

DEDICATION

Dedicated to Professor Vincenzo Balzani on the occasion of his 85th birthday.

REFERENCES

(1) Lehn, J.-M. From Molecular to Supramolecular Chemistry. In: *Supramolecular Photochemistry: Concepts and Perspectives*; ed. Wiley-VCH: Weinheim, Germany 1955, pp. 1−4.

(2) Petrov, V.; Parola, A. J.; Pina, F. Isomerization between 2-(2,4-Dihydroxystyryl)-1-Benzopyrylium and 7-Hydroxy-2-(4-Hydroxystyryl)-1-Benzopyrylium. *J. Phys. Chem. A* **2012**, *116*, 8107−8118.

(3) Pina, F.; Petrov, V.; Laia, C. A. T. Photochromism of Flavylium Systems. An Overview of a Versatile Multistate System. *Dyes Pigm.* **2012**, *92*, 877−889.

(4) Crnolatac, I.; Giestas, L.; Horvat, G.; Parola, A. J.; Piantanida, I. Flavylium Dye as Ph-Tunable Fluorescent and Cd Probe for Double-Stranded DNA and Rna. *Chemosensors* **2020**, *8*, 129.

(5) Galindo, F.; Lima, J. C.; Luis, S. V.; Melo, M. J.; Parola, A. J.; Pina, F. Water/Humidity and Ammonia Sensor, Based on a Polymer Hydrogel Matrix Containing a Fluorescent Flavylium Compound. *J. Mater. Chem.* **2005**, *15*, 2840−2847.

(6) Pina, F.; Melo, M. J.; Maestri, M.; Ballardini, R.; Balzani, V. Photochromism of 4′-Methoxyflavylium Perchlorate. A "Write-Lock-Read-Unlock-Erase" Molecular Switching System. *J. Am. Chem. Soc.* **1997**, *119*, 5556−5561.

(7) Galindo, F.; Lima, J. C.; Luis, S. V.; Parola, A. J.; Pina, F. Write-Read-Erase Molecular-Switching System Trapped in a Polymer Hydrogel Matrix. *Adv. Funct. Mater.* **2005**, *15*, 541−545.

(8) Basílio, N.; Pischel, U. Drug Delivery by Controlling a Supramolecular Host-Guest Assembly with a Reversible Photoswitch. *Chem.-Eur. J.* **2016**, *22*, 15208−15211.

(9) Romero, M. A.; Fernandes, R. J.; Moro, A. J.; Basílio, N.; Pischel, U. Light-Induced Cargo Release from a Cucurbit[8]Uril Host by Means of a Sequential Logic Operation. *Chem. Commun.* **2018**, *54*, 13335.
(10) Nogi, K.; Yorimitsu, H. Aromatic Metamorphosis: Conversion of an Aromatic Skeleton into a Different Ring System. *Chem. Commun.* **2017**, *53*, 4055−4065.
(11) Hu, G. F.; Cheng, H. B.; Niu, J. L.; Zhang, Z. H.; Wu, H. C. A Multi-Responsive Molecular Switch Based on a Diarylethene Derivative Containing Dinitrobenzenesulfonic Amide Groups. *Dyes Pigm.* **2017**, *136*, 354−360.
(12) Pu, S. Z.; Sun, Q.; Fan, C. B.; Wang, R. J.; Liu, G. Recent Advances in Diarylethene-Based Multi-Responsive Molecular Switches. *J. Mater. Chem. C* **2016**, *4*, 3075−3093.
(13) Darwish, N.; Aragones, A. C.; Darwish, T.; Ciampi, S.; Diez-Perez, I. Multi-Responsive Photo- and Chemo-Electrical Single-Molecule Switches. *Nano Lett.* **2014**, *14*, 7064−7070.
(14) Pischel, U. Chemical Approaches to Molecular Logic Elements for Addition and Subtraction. *Angew. Chem. Int. Ed.* **2007**, *46*, 4026−4040.
(15) Andreasson, J.; Pischel, U. Smart Molecules at Work-Mimicking Advanced Logic Operations. *Chem. Soc. Rev.* **2010**, *39*, 174−188.
(16) Callan, J. F.; de Silva, A. P.; Magri, D. C. Luminescent Sensors and Switches in the Early 21st Century. *Tetrahedron* **2005**, *61*, 8551−8588.
(17) De Silva, A. P.; Gunaratne, H. Q. N.; McCoy, C. P. A Molecular Photoionic and Gate Based on Fluorescent Signaling. *Nature* **1993**, *364*, 42−44.
(18) Pina, F.; Alejo-Armijo, A.; Clemente, A.; Mendoza, J.; Seco, A.; Basílio, N.; Parola, A. J. Evolution of Flavylium-Based Color Systems in Plants: What Physical Chemistry Can Tell Us. *Int. J. Mol. Sci.* **2021**, *22*, 18.
(19) Basílio, N.; Pina, F. Chemistry and Photochemistry of Anthocyanins and Related Compounds: A Thermodynamic and Kinetic Approach. *Molecules* **2016**, *21*, 25.
(20) Roque, A.; Lodeiro, C.; Pina, F.; Maestri, M.; Dumas, S.; Passaniti, P.; Balzani, V. Multistate/Multifunctional Systems. A Thermodynamic, Kinetic, and Photochemical Investigation of the 4′-Dimethylaminoflavylium Compound. *J. Am. Chem. Soc.* **2003**, *125*, 987−994.
(21) Brouillard, R.; Delaporte, B.; Dubois, J. E. Chemistry of Anthocyanins Pigments. 3. Relaxation Amplitudes in Ph-Jump Experiments. *J. Am. Chem. Soc.* **1978**, *100*, 6202−6205.
(22) Maçanita, A. L.; Moreira, P. F.; Lima, J. C.; Quina, F. H.; Yihwa, C.; Vautier-Giongo, C. Proton Transfer in Anthocyanins and Related Flavylium Salts. Determination of Ground-State Rate Constants with Nanosecond Laser Flash Photolysis. *J. Phys. Chem. A* **2002**, *106*, 1248−1255.
(23) Pina, F.; Oliveira, J.; de Freitas, V. Anthocyanins and Derivatives Are More Than Flavylium Cations. *Tetrahedron* **2015**, *71*, 3107−3114.
(24) Mendoza, J.; Basílio, N.; de Freitas, V.; Pina, F. New Procedure to Calculate All Equilibrium Constants in Flavylium Compounds: Application to the Copigmentation of Anthocyanins. *ACS Omega* **2019**, *4*, 12058−12070.
(25) McClelland, R. A.; Gedge, S. Hydration of the Flavylium Ion. *J. Am. Chem. Soc.* **1980**, *102*, 5838−5848.
(26) McClelland, R. A.; McGall, G. H. Hydration of the Flvylium Ion.2. The 4′-Hydroxyflavylium Ion. *J. Org. Chem.* **1982**, *47*, 3730−3736.
(27) Slavcheva, S.; Mendoza, J.; Stanimirov, S.; Petkov, I.; Basílio, N.; Pina, F.; Petrov, V. On the Multistate of 2′-Hydroxyflavylium-Flavanone System. Illustrating the Concept of a Timer with Reset at the Molecular Level. *Dyes Pigm.* **2018**, *158*, 465−473.
(28) Petrov, V.; Gomes, R.; Parola, A. J.; Jesus, A.; Laia, C. A. T.; Pina, F. 2′-Hydroxyflavylium: Introducing Flavanones into the Flavylium Network of Chemical Reactions. *Tetrahedron* **2008**, *64*, 714−720.
(29) Sato, S.; Kumagai, H.; Matsuba, S.; Kumazawa, T.; Onodera, J.-I.; Suzuki, M. Direct Conversion to 2-Phenyl-4-Quinolones via a 4-Alkoxyflavylium Salt from a Naturally Occurring Flavanone. *J. Heterocycl. Chem.* **1999**, *36*, 1345−1347.
(30) Petrov, V.; Diniz, A. M.; Cunha-Silva, L.; Parola, A. J.; Pina, F. Kinetic and Thermodynamic Study of 2′-Hydroxy-8-Methoxyflavylium. Reaction Network Interconverting Flavylium Cation and Flavanone. *RSC Adv.* **2013**, *3*, 10786−10794.
(31) Feringa, B. L.; Jager, W. F.; de lange, B. Organic Materials for Reversible Optical-Data Storage. *Tetrahedron* **1993**, *49*, 8267−8310.
(32) Balzani, V.; Scandola, F. *Supramolecular Photochemistry, aus Ellis Horwood Series in Physical Chemistry: Photo and Radiation Chemistry*; Ellis Horwood: New York, London, Toronto, Sydney, Tokyo, Singapore, 1991, ISBN 0-B-877531-1.
(33) Ashton, P. R.; Ballardini, R.; Balzani, V.; Boyd, S. E.; Credi, A.; Gandolfi, M. T.; GomezLopez, M.; Iqbal, S.; Philp, D.; Preece, J. A.; et al. Simple Mechanical Molecular and Supramolecular Machines: Photochemical and Electrochemical Control of Switching Processes. *Chem.-Eur. J.* **1997**, *3*, 152−170.
(34) Credi, A.; Balzani, V.; Langford, S. J.; Stoddart, J. F. Logic Operations at the Molecular Level, An Xor Gate Based on a Molecular Machine. *J. Am. Chem. Soc.* **1997**, *119*, 2679−2681.
(35) Alejo-Armijo, A.; Corici, L.; Buta, I.; Cseh, L.; Moro, A. J.; Parola, A. J.; Lima, J. C.; Pina, F. Multistate of Chemical Species of 2,6-Bis(Arylidene)Cyclohexanones. On the Role of Chalcone and Spiro Species. *Dyes Pigm.* **2020**, *174*, 7.
(36) Moro, A. J.; Pana, A. M.; Cseh, L.; Costisor, O.; Parola, J.; Cunha-Silva, L.; Puttreddy, R.; Rissanen, K.; Pina, F. Chemistry and Photochemistry of 2,6-Bis(2-Hydroxybenzilidene)Cyclohexanone. An Example of a Compound Following the Anthocyanins Network of Chemical Reactions. *J. Phys. Chem. A* **2014**, *118*, 6208−6215.
(37) Pana, A. M.; Pausescu, I.; Shova, S.; Badea, V.; Tudose, R.; Silion, M.; Costisor, O.; Cseh, L. Ph Dependent Structural Interconversion of 2-(2-Hydroxy-Benzylidene)-Cyclohexan-1-One: Crystal Structures and Spectroscopic Investigation. *J. Mol. Struct.* **2017**, *1137*, 9−16.
(38) Corici, L. N.; Shova, S.; Badea, V.; Aparaschivei, D.; Costisor, O.; Cseh, L. Investigations on the Photochromic Properties of 2,6-Bis(5-Bromo-2-Hydroxybenzylidene)Cyclohexanone. *Photochem. Photobiol. Sci.* **2017**, *16*, 946−953.
(39) Decker, H.; Felser, H. Über Cyclische Oxoniumsalze Aus Dicumarketon Und Über Spiropyranderivate. *Ber. Dtsch. Chem. Ges.* **1908**, *41*, 2997−3007.
(40) Pana, A.-M.; Badea, V.; Bănică, R.; Bora, A.; Dudas, Z.; Cseh, L.; Costisor, O. Network Reaction of 2,6-Bis(2-Hydroxybenzilidene)-Cyclohexanone by External Stimuli. *J. Photochem. Photobiol. A-Chem.* **2014**, *283*, 22−28.
(41) Moro, A. J.; Parola, A. J.; Pina, F.; Pana, A. M.; Badea, V.; Pausescu, I.; Shova, S.; Cseh, L. 2,2′-Spirobis Chromene Derivatives Chemistry and Their Relation with the Multistate System of Anthocyanins. *J. Org. Chem.* **2017**, *82*, 5301−5309.
(42) Alejo-Armijo, A.; Moro, A. J.; Parola, A. J.; Lima, J. C.; Pina, F.; Corici, L.; Shova, S.; Cseh, L. Generalization of the Anthocyanins Kinetics and Thermodynamics Multistate to 2,6-Bis(2-Hydroxybenzylidene)Cyclohexanones. *Dyes Pigm.* **2019**, *163*, 573−588.
(43) Alejo-Armijo, A.; Corici, L.; Cseh, L.; Aparaschivei, D.; Moro, A. J.; Parola, A. J.; Lima, J. C.; Pina, F. Achieving Complexity at the Bottom. 2,6-Bis(Arylidene) Cyclohexanones and Anthocyanins: The Same General Multistate of Species. *ACS Omega* **2018**, *3*, 17853−17862.
(44) Jurd, L. Anthocyanins and Related Compounds. I. Structural Transformations of Flavylium Salts in Acidic Solutions. *J. Org. Chem.* **1963**, *28*, 987−991.
(45) Jurd, J. Rearrangements of 5,8-Dihydroxyflavylium Salts. *Chem. & Ind.* **1962**, 1197−1198.
(46) Jurd, L. H.; Harborne, J. B. The Structure of Aurantinidin. *Phytochemistry* **1968**, *7*, 1209−1211.
(47) Bjorøy, Ø.; Rayyan, S.; Fossen, T.; Andersen, Ø. M. Structural Properties of Anthocyanins: Rearrangement of C-Glycosyl-3-Deoxyanthocyanidins in Acidic Aqueous Solutions. *J. Agric. Food Chem.* **2009**, *57*, 6668−6677.

https://doi.org/10.1021/acsomega.1c04456
ACS Omega 2021, 6, 30172−30188

(48) Cruz, L. M.; Basilio, N. M.; de Freitas, V. A.; Lima, J. C.; Pina, F. J. Extending the Study of the 6,8 Rearrangement in Flavylium Compounds to Higher Ph Values: Interconversion between 6-Bromo and 8-Bromo-Apigeninidin. *Chemistryopen* **2016**, *5*, 236−246.
(49) Basílio, N.; Lima, J. C.; Cruz, L.; de Freitas, V.; Pina, F.; Ando, H.; Kimura, Y.; Oyama, K.-I.; Yoshida, K. Unveiling the 6,8-Rearrangement in 8-Phenyl-5,7-Dihydroxyflavylium and 8-Methyl-5,7-Dihydroxyflavylium through Host-Guest Complexation. *Eur. J. Org. Chem.* **2017**, *2017*, 5617−5626.
(50) Basilio, N.; Cruz, L.; de Freitas, V.; Pina, F. A Multistate Molecular Switch Based on the 6,8-Rearrangement in Bromo-Apigeninidin Operated with Ph and Host- Guest Inputs. *J. Phys. Chem. B* **2016**, *120*, 7053−7061.
(51) Cao, L.; Šekutor, M.; Zavalij, P. Y.; Mlinarić-Majerski, K.; Glaser, R.; Isaacs, L. Cucurbit[7]Uril.Guest Pair with an Attomolar Dissociation Constant. *Angew. Chem., Int. Ed.* **2014**, *53*, 988−993.

NOTE ADDED AFTER ASAP PUBLICATION

The uncorrected version was published October 13, 2021; the corrected version reposted on October 15, 2021.

https://doi.org/10.1021/acsomega.1c04456
ACS Omega 2021, 6, 30172−30188